CAL SOCIETY

MEMOIRS

OF THE

COLLEGE OF SCIENCE

KYOTO IMPERIAL UNIVERSITY

SERIES A

VOL. XVIII, NO. 1

JANUARY 1935

KYOTO

1127 29

On the Group of Zero-Sequence

By

Toshizô Matsumoto

(Received November 9, 1934)

1. Given a sequence of an infinite number of real numbers, $\{u_\nu\}$, we rearrange its terms by the substitution

$$S \equiv \begin{pmatrix} u_1 & u_2 & \cdots\cdots & u_\nu & \cdots\cdots \\ u_{s_1} & u_{s_2} & \cdots\cdots & u_{s_\nu} & \cdots\cdots \end{pmatrix},$$

or more simply by

$$S \equiv \begin{pmatrix} 1 & 2 & \cdots\cdots & \nu & \cdots\cdots \\ s_1 & s_2 & \cdots\cdots & s_\nu & \cdots\cdots \end{pmatrix}$$

where the transformed sequence is $\{u_{s_\nu}\}$. If the series $\sum_{\nu=1}^{\infty}(u_\nu - u_{s_\nu})$ be absolutely convergent, then we say the sequence $\{u_\nu\}$ admits the substitution S. The totality of all such substitutions forms the group of the sequence $\{u_\nu\}$. If the sequence be a zero-sequence, i. e., if $\lim_{\nu\to\infty} u_\nu = 0$, then the group of the sequence $\{u_\nu\}$ is also called the group of the series (convergent or divergent)

$$\sum u_\nu \equiv u_1 + u_2 + \cdots\cdots + u_\nu + \cdots\cdots .^{1}$$

In this note we shall consider only zero-sequences. A group is said to be admitted by a sequence provided all its substitutions are admitted by the sequence. Such a group is a subgroup of the group of the sequence.

2. If $\sum u_\nu$ be absolutely convergent, then it admits all possible substitutions, i. e., the symmetric group. Conversely

1. Toshizô Matsumoto. Group-theory of semi-convergent series. These Memoirs, X, No. 5 (1927)
„ Group-theory of sequences of numbers. *Ibid*, XI, No. 1 (1928)
„ On the decomposition of substitutions of groups of sequences, *Ibid*, XIII, No. 2 (1930)

If the sequence $\{u_\nu\}$ *admits the symmetric group, then the series* $\sum u_\nu$ *is absolutely convergent.*

I enunciated this theorem in my first paper without proof. When the sequence $\{u_\nu\}$ has an infinite number of terms of both signs, it is evident.[1] In the other case, we may suppose $u_\nu > 0$, $\nu = 1, 2, \ldots\ldots$ without loss of generality. Since $u_\nu \to 0$, it gives a partial sequence $\{u_{n_\nu}\}$ such that $\sum u_{n_\nu}$ is convergent. Let $\{u_{m_\nu}\}$ be the sequence with terms remaining in $\{u_\nu\}$ after the rejection of u_{n_ν}, $\nu = 1, 2, \ldots$. Then $\sum u_{m_\nu}$ must be divergent, or else $\sum u_\nu$ would be convergent. Now by the substitution

$$(m_1\ n_1)(m_2\ n_2)\ldots\ldots(m_\nu\ n_\nu)\ldots\ldots$$

the series of the differences of the absolute values of the corresponding terms will be

$$2\sum |u_{m_\nu} - u_{n_\nu}| \geqslant 2(\sum u_{m_\nu} - \sum u_{n_\nu}) = \infty.$$

This contradicts the hypothesis; so that the series $\sum u_\nu$ must be convergent.

If $\{u_\nu\}$ is not a zero-sequence, the theorem is not true.[2]

3. If the sequence $\{u_\nu\}$ admits the substitution $S \equiv \binom{\nu}{s_\nu}$ i. e., if the series $\sum |u_\nu - u_{s_\nu}|$ eb convergent, the series $\sum ||u_\nu| - |u_{s_\nu}||$ is *a fortiori* convergent. Therefore the sequence $\{|u_\nu|\}$ admits the substitution S. Hence the group of $\{u_\nu\}$ is a subgroup of that of $\{|u_\nu|\}$.

We shall consider in the following the *positive zero-sequences*, i. e., those whose terms are all positive and tend to zero.

4. *Let* $\{u_\nu\}$ *be a positive zero-sequence, then the group of* $\{u_\nu\}$ *is a proper subgroup (divisor) of that of the sequence* $\{u_\nu^\rho\}$, $(\rho > 1)$, in so far as the series $\sum u_\nu$ is divergent.

Let the substitution $S \equiv \binom{\nu}{s_\nu}$ be any substitution admitted by the sequence $\{u_\nu\}$, it can easily be seen that the sequence $\{u_\nu^\rho\}$ also admits S. For let A be the upper bound of the sequence $\{u_\nu\}$, then

$$|u_\nu^\rho - u_{s_\nu}^\rho| < \rho A^{\rho-1} |u_\nu - u_{s_\nu}|, \quad (\rho > 1).$$

Hence the series $\sum |u_\nu^\rho - u_{s_\nu}^\rho|$ is convergent, since by hypothesis the series $\sum |u_\nu - u_{s_\nu}|$ is convergent.

To prove that there is a substitution admitted by $\{u_\nu^\rho\}$, but not by $\{u_\nu\}$, $\sum u_\nu$ being divergent, at first we note that if $A_1, A_2, \ldots A_n$ be positive, then for any number $\lambda > 1$, we have the inequality

1. *Loc. cit.*, the first paper, p. 220.
2. *Loc. cit.*, the second paper, p. 12.

$$A_1^\lambda + A_2^\lambda + \ldots + A_n^\lambda < (A_1 + A_2 + \ldots + A_n)^\lambda.$$

Now choose some terms of $\{u_\nu\}$ (in the order of increasing indeces) such that

$$1 \geqslant u_{11} + u_{12} + \ldots + u_{1k_1} > \frac{1}{2},$$

where $u_{11}, u_{12}, \ldots, u_{1k_1}$ are certain terms of $\{u_\nu\}$, only the notations of the indeces being changed. This is always possible, since $u_\nu \to 0$ and $\sum u_\nu = \infty$. Again we may choose some terms from the remaining terms of $\{u_\nu\}$ such that

$$\frac{1}{2} \geqslant u_{21} + u_{22} + \ldots + u_{2k_2} > \frac{1}{3},$$

$$\ldots\ldots\ldots\ldots\ldots\ldots\ldots\ldots\ldots\ldots$$

$$\frac{1}{n} \geqslant u_{n1} + u_{n2} + \ldots + u_{nk_n} > \frac{1}{n+1},$$

$$\ldots\ldots\ldots\ldots\ldots\ldots\ldots\ldots\ldots\ldots$$

In choosing these terms we may assume that

$$k_1 \leqslant k_2 \leqslant \ldots\ldots \leqslant k_n \leqslant \ldots\ldots$$

For after $u_{11}, u_{12}, \ldots, u_{1k_1}$ is chosen, we choose the next group of such terms $u_{21}, u_{22}, \ldots, u_{2k_2}$ among the remaining terms of $\{u_\nu\}$ as

$$k_1 u_\nu \leqslant \frac{1}{2}.$$

This is possible since $u_\nu \to 0$. Then we have

$$u_{21} + u_{22} + \ldots + u_{2k_1} \leqslant k_1 \times \frac{1}{2k_1} = \frac{1}{2};$$

and we add some terms if necessary so that

$$\frac{1}{2} \geqslant u_{21} + u_{22} + \ldots + u_{2k_2} > \frac{1}{3}.$$

This is possible since $u_\nu \to 0$ and $\sum u_\nu = \infty$. Therefore

$$k_2 \geqslant k_1.$$

This consideration is quite general. So we may suppose that

$$k_1 \leqslant k_2 \leqslant \ldots\ldots \leqslant k_n \leqslant \ldots\ldots$$

Now put for simplicity

$$U_n \equiv u_{n1} + u_{n2} + \ldots + u_{nk_n},$$

$$U_n' \equiv u_{n1}^\rho + u_{n2}^\rho + \ldots + u_{nk_n}^\rho, \quad n = 1, 2, \ldots\ldots$$

Then by the inequality remarked above

$$U_n^\rho = (u_{n1} + u_{n2} + \ldots + u_{nk_n})^\rho$$

$$> u_{n1}^\rho + u_{n2}^\rho + \ldots + u_{nk_n}^\rho = W_n^\rho.$$

Since $\frac{1}{n} \geqslant U_n$ and hence $\frac{1}{n^\rho} \geqslant U_n^\rho$, we have

$$\frac{1}{n^\rho} > W_n^\rho.$$

Thus we see the series $\sum_{n=1}^{\infty} U_n$ is divergent while the series $\sum_{n=1}^{\infty} W_n^\rho$ is convergent.

Now since $U_n \to 0$, we may take a partial sequence $\{U_{n_i}\}$ in order from $\{U_n\}$ such that the series

$$U_{n_1} + U_{n_2} + \ldots + U_{n_i} + \ldots\ldots$$

is convergent. Here we may suppose that

$$n_1 > 1, \quad n_2 > n_1 + 1, \ldots, \quad n_{i+1} > n_i + 1, \ldots;$$

for the sequence $\{U_n\}$ is monotone decreasing, and to select a convergent series, a smaller U_n, i. e., U_n with a greater index is more effective. Let $\{U_{m_i}\}$, $(m_1 = 1)$, be the remaining sequence in order, then the series

$$U_{m_1} + U_{m_2} + \ldots + U_{m_i} + \ldots\ldots$$

is divergent, since $\sum U_n = \sum U_{m_i} + \sum U_{n_i} = \infty$. By our choice of n_1, $n_2, \ldots\ldots$, we have

$$m_i < n_i, \quad i = 1, 2, \ldots\ldots$$

Therefore the number of terms in U_{m_i} is not greater than that in U_{n_i} i. e.,

$$k_{m_i} \leqslant k_{n_i}, \quad i = 1, 2, \ldots\ldots$$

Now put

$$U'_{n_i} \equiv u_{n_i 1} + u_{n_i 2} + \ldots + u_{n_i k_{m_i}},$$

then since

$$U'_{n_i} \leqslant U_{n_i}, \quad i = 1, 2, \ldots\ldots$$

the series $U'_{n_1} + U'_{n_2} + \ldots + U'_{n_i} + \ldots\ldots$

is also convergent. Now consider the substitutions

$$T_1 \equiv (u_{m_1 1}, u_{n_1 1}) \ldots\ldots (u_{m^i k_{m_i}}, u_{n_i k_{m_i}}),$$

$$(i = 1, 2, \ldots\ldots)$$

$$T \equiv T_1 T_2 \ldots\ldots T_i$$

The series of the absolute values of differences of corresponding terms of the sequence $\{u_\nu\}$ and its transformed one by T is

$$2\sum_{i=1}^{\infty}\{|u_{m_i 1}-u_{n_i 1}|+\ldots+|u_{m_i k_{m_i}}-u_{n_i k_{m_i}}|\}$$
$$\geqslant 2\sum_{i=1}^{\infty}(U_{m_i}-U_{n_i})=\infty.$$

Thus the sequence $\{u_\nu\}$ does not admit the substitution T.

On the other hand

$$2\sum_{i=1}^{\infty}\{|u^{\rho}_{m_i 1}-u^{\rho}_{n_i 1}|+\ldots+|u^{\rho}_{m_i k_{m_i}}-u^{\rho}_{n_i k'_{m_i}}|\}$$
$$<2\sum_{i=1}^{\infty}(W_{m_i}+W_{n_i}).$$

This is convergent, since $\sum_{n=1}^{\infty}W_n$ is convergent.

Thus we see there is at least a substitution T in the group of the sequence $\{u^{\rho}_\nu\}$ which is not admitted by the sequence $\{u_\nu\}$. We conclude therefore the group of $\{u_\nu\}$ is a proper subgroup of that of $\{u^{\rho}_\nu\}$, $(\rho>1)$.

5. We would conjecture that the group of $\{u_\nu\}$ is a normal subgroup of that of $\{u^{\rho}_\nu\}$, $(\rho>1)$. But this is not true. For as we have proved there is a partial sequence, say, $\{u_{n_i}\}$ of $\{u_\nu\}$ such that $\sum u_{n_i}$ is divergent while $\sum u^{\rho}_{n_i}$ is convergent. Hence suppose from the beginning that $\sum u_\nu$ is divergent while $\sum u^{\rho}_\nu$ is convergent, $(\rho>1)$, then clearly it gives a cycle, say

$$C\equiv(\ldots\ldots c_{-2}\ c_{-1}\ c_1\ c_2\ldots\ldots)$$

admitted by the sequence $\{u_\nu\}$ where $c_1, c_{-1}\ c_2, c_{-2},\ldots\ldots$are as a whole equal to 1, 2, 3, 4,..... Also we can easily construct a cycle, say

$$D\equiv(\ldots\ldots d_{-2}\ d_{-1}\ d_1\ d_2\ldots\ldots)$$

not admitted by the sequence $\{u_\nu\}$, where $d_1, d_{-1}, d_2, d_{-2},\ldots\ldots$are as a whole equal to 1, 2, 3, 4,..... Now put

$$T\equiv\begin{pmatrix} c_1 & c_{-1} & c_2 & c_{-2}\ldots\ldots \\ d_1 & d_{-1} & d_2 & d_{-2}\ \ldots\ldots \end{pmatrix}.$$

Since $\sum u^{\rho}_\nu$ is convergent, $\{u^{\rho}_\nu\}$ admits T, and

$$T^{-1}CT=D$$

which is not admitted by $\{u_\nu\}$. It is clear that T is not admitted by $\{u_\nu\}$ or else D should be admitted by it. Therefore the group of $\{u_\nu\}$ cannot be a normal subgroup of that of $\{u^{\rho}_\nu\}$, $(\rho>1)$.

6. We may extend the theorem proved in N°4 to the sequences $\{\varepsilon_\nu u_\nu\}$ and $\{\varepsilon_\nu u_\nu^\rho\}$, $(\rho>1)$ where $\{u_\nu\}$ is as before a positive zero-sequence and ε_ν is $+1$ or -1. It is clear that the group of $\{\varepsilon_\nu u_\nu\}$ is a subgroup of that of $\{\varepsilon_\nu u_\nu^\rho\}$. For by $S\equiv\binom{\nu}{s_\nu}$, let $\sum|\varepsilon_\nu u_\nu-\varepsilon_{s_\nu}u_{s_\nu}|$ be convergent, then since $u_\nu\to 0$, considering only the terms that u_ν, u_{s_ν} are sufficiently small, $(u_\nu,\ u_{s_\nu}<e^{-1})$, the series $\sum|\varepsilon_\nu u_\nu^\rho-\varepsilon_{s_\nu}u_{s_\nu}^\rho|$ is also convergent. This can easily be shown by the method of maximum and minimum Since $\sum u_\nu$ is supposed to be divergent, there is a partial sequence $\{\varepsilon_{n_i}u_{n_i}\}$ of $\{u_\nu\}$ whose terms are of the same sign and $\sum\varepsilon_{n_i}u_{n_i}$ is divergent. Applying the theorem of N°4 to the sequences $\{\varepsilon_{n_i}u_{n_i}\}$ and $\{\varepsilon_{n_i}u_{n_i}^\rho\}$ we may conclude that

The group of the zero-sequence $\{\varepsilon_\nu u_\nu\}$ *is a proper subgroup of that of the sequence* $\{\varepsilon_\nu u_\nu^\rho\}$, $(\rho>1)$.

This subgroup is not a normal subgroup. The following example is to be noted.

$$\{\varepsilon_\nu u_\nu\}\equiv\left\{(-1)^{\nu-1}\frac{1}{\nu}\right\},$$

$$\{\varepsilon_\nu u_\nu^\rho\}\equiv\left\{(-1)^{\nu-1}\frac{1}{\nu^\rho}\right\},\quad(\rho>1)$$

$$S\equiv(1\ 3)(4\ 6)(7\ 9)\cdots\cdots(3n-2\ 3n)\cdots\cdots,$$
$$T\equiv(1\ 2)(4\ 5)(7\ 8)\cdots\cdots(3n-2\ 3n-1)\cdots\cdots$$

Since the series $\sum(-1)^{\nu-1}\frac{1}{\nu^\rho}$ is absolutely convergent, it admits the symmetric group; while the sequence $\left\{(-1)^{\nu-1}\frac{1}{\nu}\right\}$ admits the substitution S but not the substitution T. Now

$$\begin{aligned}T^{-1}ST=&(1\ 2)(1\ 3)(1\ 2)\times(4\ 5)(4\ 6)(4\ 5)\times(7\ 8)(7\ 9)(7\ 8)\\&\times\cdots\cdots\cdots\cdots\cdots\\&\times(3n-2\ 3n-1)(3n-2\ 3n)(3n-2\ 3n-1)\times\cdots\cdots\\=&(2\ 3)(5\ 6)(8\ 9)\cdots(3n-1\ 3n)\cdots\cdots\end{aligned}$$

and this is not admitted by $\left\{(-1)^{\nu-1}\frac{1}{\nu}\right\}$.

7. *Let* $\{u_\nu\}$ *and* $\{v_\nu\}$ *be two zero-sequences (not necessarily positive), such that for any two indeces* ν, μ *we have either* $u_\nu\geqq u_\mu$ *and* $v_\nu\geqq v_\mu$ *at the same time or* $u_\nu\leqq u_\mu$ *and* $v_\nu\leqq v_\mu$ *at the same time, then the set of all substitutions admitted by* $\{u_\nu\}$ *and* $\{v_\nu\}$ *at the same time forms a group.*

For let $S\equiv\binom{\nu}{s_\nu}$ be admitted by $\{u_\nu\}$ and $\{v_\nu\}$ at the same time, i. e., $\sum|u_\nu-u_{s_\nu}|$ and $\sum|v_\nu-v_{s_\nu}|$ be convergent, then since

$$\sum|(u_\nu+v_\nu)-(u_{s_\nu}+v_{s_\nu})|$$
$$=\sum\{|u_\nu-u_{s_\nu}|+|v_\nu-v_{s_\nu}|\},$$

the sequence $\{u_\nu+v_\nu\}$ also admits the substitution S. Conversely any substitution admitted by $\{u_\nu+v_\nu\}$ is also admitted by $\{u_\nu\}$ and $\{v_\nu\}$ at the same time. The set of all substitutions admitted by $\{u_\nu+v_\nu\}$ forms a group. Hence the set of all substitutions common to both groups of $\{u_\nu\}$ and $\{v_\nu\}$ forms a group.

Digitized by the Internet Archive
in 2024

https://archive.org/details/memoirs-faculty-science-kyoto-phys-astro-geophys-chem_1935-01_18_1

Melting of Metal-Crystals at their Boundaries, and a Theory of Recrystallization of Metals

By

Usaburo Yoshida and Kazuo Koyanagi

(Received November 18, 1934)

Abstract

It is found that when the temperature of a metal is raised to a value just below its melting point, the metal melts at its crystal-boundaries. Next, by assuming that the metal melts at its crystal-boundaries in its recrystallization-temperature, a theory of the recrystallization of metals is proposed.

Melting of Metal-Crystals at their Boundaries

When the writers were endeavouring to get large single crystal plates of aluminium by the stress-annealing method, it happened rather accidentally that the recrystallizing temperature in the furnace was just below the melting point of aluminium (657°C). When the aluminium plates were taken out from the furnace, after a prolonged exposure to such temperature, the writers noticed that the surfaces of the plates were engraved with a zigzag network of shallow and thin grooves. This indicates that the aluminium was melted at these grooves. Next, the surfaces of the plates were etched by some reagent, and it was confirmed that the grooves were nothing but the boundaries of the single crystals of aluminium. This shows that the aluminium crystals are easier to melt at their boundaries

The furnace used in the present experiment was a resistance type, consisting of a porcelain tube about one metre in length and five cms. in diameter and a nichrome wire wound uniformly around the former. The furnace was set vertically, and some long test pieces of metal plates of suitable size were hung in the middle part of the porcelain tube of the furnace. Though the temperature would be nearly uniform in the middle part of the tube, it would not be exactly so. The

temperature in the furnace is of course governed by the electric current passing through the nichrome wire. And though it is very difficult at a definite point in the furnace to keep the temperature just at or just below the melting point of the metal by the regulation of the electric current, this difficulty is not met with at the place in the furnace occupied by the specimens, as the present furnace has some non-uniform temperature-distribution. Assisted by such circumstances the writers could succeed in raising the temperature of the specimens just below the melting point of aluminium or that of some other metal, at least at some parts of them.

Some of the photographs of the surfaces of the metal plates exposed to such temperature for a long time are reproduced in Plate I. In the case of Figs. 1a and 1b in Plate I, a commercial aluminium plate having the size $39 \times 3 \times 0.1$ cm^3 was first annealed at the temperature of about 390°C for 80 hours, next it was elongated by 1.25% of its original length, and then it was subjected to the temperature just below the melting point of aluminium for about 70 hours. A zigzag network of thin and shallow grooves engraved on the surface of the plate in this case will be seen clearly in Fig. 1a, Plate I. The width and the depth of the grooves are estimated to be of the order of 0.1–0.3 mm. in this case. Next the same part of the aluminium plate is etched by hydrochloric acid, and its photograph is shown in Fig. 1b. By comparing these two photographs it will be clear now that the thin and shallow grooves engraved on the surface of the aluminium plate are nothing but the boundaries of single crystals of aluminium. This point was confirmed to be so with nearly all the specimens prepared similarly, which amounted to more than one hundred in all. However it occured rarely that the crystal boundary did not coincide exactly with the groove. This seems, in all probability, to be due to the growth of a crystal across the groove in the cooling state after the formation of the groove at the crystal boundary.

Thus the coarseness of the network of the grooves depends generally upon the size of the crystals. As is well known, the metal crystals produced by recrystallization in a piece of a metal which has not been subjected to any slight preliminary elongation, do not grow much. Consequently the network of the grooves engraved on the surface of such metal ought to be fine. A commercial aluminium plate, without any preliminary annealing and elongation, was directly exposed to the temperature just below its melting point for about two days.

The appearance of the surface of the plate thus prepared is shown by Fig. 2, Plate I, and it reveals clearly a fine network of the grooves as is expected.

The fact that the grooves are formed at the crystal boundaries will still clearly be seen in Figs. 3_a and 3_b in Plate I. Fig. 3_a shows the etched surface of a single crystal plate of aluminium prepared by ordinary stress-annealing method. The recrystallization temperature in this case was lower by about fifty degrees than the melting point of aluminium, and any trace of the grooves could not be detected at the crystal boundaries by the naked eye. Next the same specimen was subjected to the temperature just below the melting point of aluminium for about twenty hours, and then comparatively deep and wide grooves were formed at the crystal boundaries. The etched surface of the specimen thus prepared is shown in Fig. 3_b in the plate. By comparing Figs. 3_a and 3_b it will clearly be seen that the crystals did not grow further and the grooving occurred exactly at the crystal boundaries by the second recrystallizing treatment. Here it must be noted that one portion in Fig. 3_b, which looks like a single crystal formed by the unification of two neighbouring single crystals in Fig. 3_a, is not really single but is composed of the same two crystals seen in Fig. 3_a. The cause of this ambiguity is nothing but an improper illumination of the specimen in taking its photograph. With the actual specimen no doubt is left on this point.

It is already stated that the grooves at the crystal boundaries are formed by the melting of the metal there. This consideration will be strengthened by the following instances. Once it occurred to the writers, with comparatively long aluminium plate and with sufficiently high temperature of the furnace which was able to form deep grooves, that the lower part of the plate fell down to the bottom of the furnace, by being separated from the upper part of the plate at their crystal boundary ; and moreover that the fallen lower part was nearly broken at the crystal boundaries into several pieces. Still it occurred to the writers, with sufficiently high temperature which was able to form deep grooves, that a whole single crystal formed in an aluminium plate slipped a little from one side of the plate to the other. These instances show clearly that the metal became soft at the crystal boundaries in consequence of the melting of the metal there.

It is already stated that the temperature in the furnace used in the present experiment is not exactly uniform, but a little different

according to the position in the furnace. In a long furnace such as employed by the present experiment the temperature will become gradually lower from the maximum in the middle towards each end. As in the case of the specimen shown by Fig. 3_b in Plate I, the lower end of the specimen reached nearly to the middle of the furnace, the temperature was expected to become higher gradually from the upper part of the specimen to its lower part. The lower end of the specimen was melted as a whole in this case, as seen in Fig. 3_b; therefore the temperature of the specimen is supposed to become lower toward its upper end from the melting point of aluminium at its lower end. According to this temperature distribution the grooves formed at the crystal boundaries became thinner gradually toward the upper end. This fact that the grooves become thicker as we approach to the melting point of aluminium was confirmed by the writers with more than 30 specimens.

The question why the crystal boundaries become grooved by melting is not clear yet; but so far as the writers have experienced three following causes seems to be conceivable. 1) Single crystal pieces are displaced a little differently by gravity. 2) The melted part at the crystal boundaries is evaporated more strongly than at other places. 3) The molten part at the crystal boundaries flows downward by gravity. Among these three causes the third one seems to be very rare, and it happens only when the groove is pretty thick. It is seldom, too, that we can detect clearly that the grooving is due to the first cause. Consequently the second cause, i. e. the evaporation of the metal, seems to be the most predominant factor in forming the groove at the melted crystal boundaries

As to the lowering of the melting point at the crystal boundaries two causes seems to be conceivable. 1) Accumulation of some impurities at the crystal boundaries. 2) It is a proper nature of the metal itself that it is easier to melt at its crystal boundaries even when there is no accumulation of the impurities. If we assume that, in recrystallizing the metal, the impurities contained in the metal are displaced to the crystal boundary, the accumulation of the impurities must be located in a very thin sheet at this boundary. Thus if we assume that the melting of the metal at its crystal boundaries is due to the first cause, the groove formed by the melting of the metal should be correspondingly thin always. However this does not accord with the actual observation, as the width of the groove sometimes attains to

one or more than one millimetre, as seen in Fig. 3_b or in Figs. 4_a and 4_b in Plate I. Next the writers repeated the same experiment as before with pure aluminium plate (99.8% Al+0.08% Si+0.12% Fe+ x% O_2), and it was confirmed that the network of the grooves was also produced at the crystal boundaries similarly as with commercial aluminium plate. Such grooves obtained with pure aluminium plates are shown in Figs, 4_a and 4_b in Plate I. Here Fig. 4_a represents the appearance of the unetched surface, and Fig. 4_b that of the etched surface.

The melting of the metal at its crystal boundaries just below its melting point is not confined to aluminium. The writers carried out similar experiments with commercial plates of tin and zinc, and the network of the grooves formed by the melting of the metal at its crystal boundaries was respectively observed with these two metals. The grooves formed on the surface of a tin plate are represented in Figs. 5_a and 5_b in Plate I: where Fig. 5_a shows the unetched surface and Fig. 5_b the etched surface. Considering thus it seems not to be unnatural to conclude that the melting of the metal at its crystal boundaries at a temperature below its melting point is a universal nature of the metals.

A Theory of the Recrystallization of Metals

It is already stated that when a metal is subjected for a long time to its recrystallization temperature which is very near to its melting point the grooves formed by the melting of the metal at its crystal boundaries become thinner as the recrystallization temperature decreases. Though, when the recrystallization temperature is still lowered, any trace of the grooves can not be detected at the crystal boundaries, still it seems not to be unnatural to suppose that the metal is melted by very thin layers at its crystal boundaries even in such a case; and standing on this assumption the writers attempted to establish a theory of recrystallization of metals.

It is already stated too that when the recrystallization temperature is just below the melting point of the metal, the width of the grooves formed by the melting of the metal at its crystal boundaries attains sometimes to one or more than one millimetre. This seems to indicate that the crystal is easier to melt not only at its crystal boundaries but also at the contact surface of the metal crystal with its melt than at the interior of the crystal. Moreover the writers assume that the

distorted metal crystal is easier to melt than that without any distortion. This assumption is somewhat different from that of Tarschisch[1], who proposed a theory of recrystallization of metals by assuming that the metal is easier to melt at the part where interatomic distances became larger by deformation, and that the crystal nuclei are formed in the part thus melted. However the second assumption made by Tarschisch that in the course of recrystallization the crystal nuclei are formed in the melted part of the metal seems to be supported at least to a certain degree by the investigation made by K. Tanaka[2] on the recrystallization of slightly deformed single crystals of aluminium. According to him, the orientation of the micro-crystals produced by a slight deformation of a single crystal of aluminium is not much different from that of the mother single crystal, and the orientation of the crystals formed by recrystallizing such slightly deformed single crystal is independent of the orientation of the micro-crystals in a slightly deformed single crystal of aluminium. Thus, as to the formation of the recrystallization nucleus, the writers assume with Tarschisch that the nucleus is formed in the melted part of the metal.

Now, relying upon the considerations stated above, let us consider the mechanism of the recrystallization of metals. When a metal is deformed by some mechanical treatment, the metal crystals are smashed into finer micro-crystals ; and these micro-crystals are a little distorted, in other words they are strained, resulting to the lowering of their melting point. Next when such a metal is subjected to a recrystallization temperature, the metal will melt at the boundaries of the micro-crystals by very thin layers, and then undistorted perfect crystals will be formed in the melts as the recrystallization nuclei, whose melting point is higher than that of the distorted micro-crystals. By such difference of the melting point between distorted and undistorted crystals, the recrystallization nuclei will grow gradually by the crystallization of the melts on their surfaces, and the distorted micro-crystals will melt correspondingly at their boundaries, resulting in the growth of the new undistorted crystals by the consumption of the distorted micro-crystals. Thus when all the distorted micro-crystals are consumed and the whole metal piece is occupied by new undistorted crystals the recrystallization process actually comes to an end ; because the stability as a solid is the same for all the new undistorted crystals.

1. Tarschisch : Phys. Z. S., **35**, 469 (1934)
2. Tanaka : These Memoirs, **11**, 229 (1928)

It seems natural to consider that the degree of the lowering of the melting point of a distorted metal crystal depends directly upon the magnitude of the distortion or strain, and the melting point will decrease with increasing distortion. Thus when a metal is strongly deformed the locations in the metal where the micro-crystals suffer the strains of more than a certain value become numerous, i. e. the recrystallization nuclei become numerous, and the crystals formed by recrystallization become smaller in size. However when the deformation of the metal is small, for example one or two percent elongation as in the case of obtaining large single crystals by recrystallization method, the locations in the metal where the micro-crystals suffer the strains of more than a certain value become rare; i. e. the number of the recrystallization nuclei become rare, and thus the crystals obtained by the recrystallization process become larger.

As is stated above, the writers assumed that the melting point of a metal crystal depends upon the strain it suffers. Though this consideration appears to be inconsistent with the fact that a metal has a definite melting point, actually it is not so. When the temperature of a deformed metal is increased gradually up to its melting point, all the distorted metal crystals will be replaced by new undistorted metal crystals by the recrystallization process before the temperature reaches to the melting point of the metal. Thus when the melting point of the metal is reached, the melting is not from initial distorted crystals but from new undistorted crystals to the liquid. Reversely in the solidifying state of a metal from its melt to its crystals, undistorted metal crystals formed by solidification are in contact with its melt. Considering in such a way, the actual melting point of a metal is nothing but the temperature at which the undistorted metal crystal is in contact with its melt, which is definite and proper to the undistorted crystals of the metal.

Till now the writers stated a theory of recrystallization of the metal, which stands on the consideration that the metal melts at its crystal boundaries at its recrystallization temperature. This consideration was confirmed to be so only at the temperature just below the melting point of the metal, and for a recrystallization temperature still lower than this it is no more than a hypothesis. However if this is an actual phenomenon, it will have an important bearing on various properties of the metals. For an example, such phenomenon as intermetallic diffusion may be caused by the melting of the metals at their crystal boundaries.

In conclusion the writers wish to express their hearty thanks to Professor D. Uno of the Metallographical Department for his kindness in furnishing the specimen of pure aluminium to the writers.

Plate I

2 ×

Fig. 1a

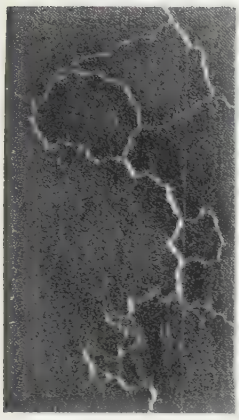

Fig. 1b

Fig. 2

1.3 ×

Fig. 4a

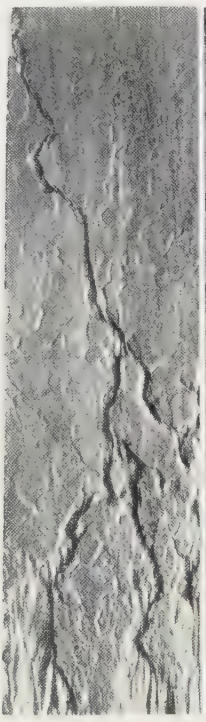

Fig. 4b

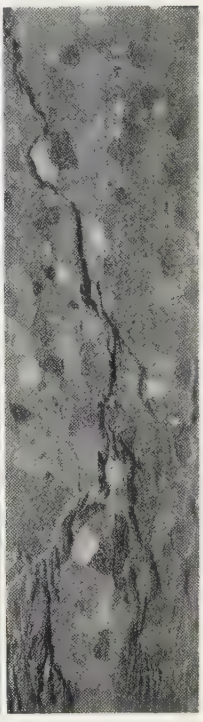

Fig. 3a

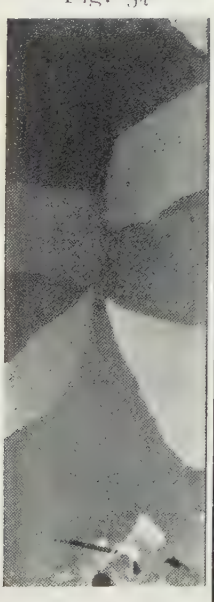

Fig. 3b

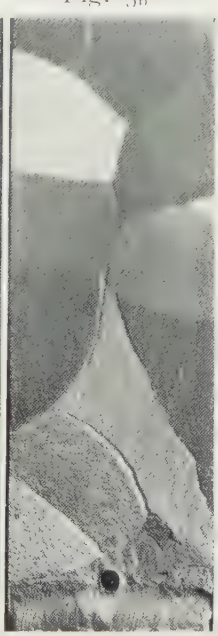

2 ×

Fig. 5a

Fig. 5b

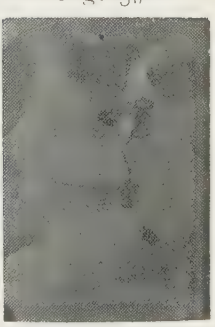

On the Crystal Structure and Crystalline Configuration of the Normal and Modified Si-Al Alloys

By

Hajime Kotô

(Received November 18, 1934)

Abstract

The cooling curves and the micro-structures of various sand-cast specimens were preliminarily examined in connection with the normal and modified Si-Al alloys, to find out the characteristic modifying effects of a series of substances analogous in some peculiar respects to sodium. By way of revising and completing the conclusion thus arrived at, the X-ray investigation was then carried out, in connection with the crystal structures and the crystalline configurations of the same alloys.

As the consequence of these researches, it became clear on the one hand, that the micro-structures of the alloys inform us very little with regard to their actual crystalline configurations: Moreover, on the other hand, the peculiarities of the substances efficacious for the modification of Si-Al alloy, were confirmed not always to be in good accordance with those generally accepted, by the present theories of modification.

Introduction

The marked increase of the industrial importance of Si-Al alloys during the last few years is mainly due to the improvement in their mechanical properties, caused by the modifying process of adding a small quantity of sodium or sodium fluoride. Accordingly, a number of metallographical investigations by means of the thermal analysis and microscopical test have hitherto been made to find out the reason why such a modification should take place. The crystal structures and crystalline configurations of Si-Al alloys were also examined by Jeffries,[1] Shinoda[2] and others utilizing X-rays, and as the consequences

1. Chem. and Met. Eng., **29**, 360 (1922)
2. Suiyokwai-Shi, Department of Mining and Metallurgy, Kyoto Imperial University, No. 5, **5** (1927)

of these X-ray examinations, the mechanism of modification above stated was in certain respects conclusively demonstrated.

Notwithstanding these, there remains still unknown with regard to this subject, even whether or not the micro-structures of the alloys are really in good accordance with their actual crystalline configurations; much more are further experiments needed to arrive at a general conclusion. Owing to such a lack of evidences, the mechanism of modification of Si-Al alloys, which has generally been attributed to the formation of ternary constituents or under-cooling phenomenon by the present thermodynamical considerations, seems hardly to be explainable in terms of the crystallographical theory of the space-lattice. So, the writer was induced to carry out the present investigation, not only by way of continuing the foregoing researches on the growth of metallic crystals[1] or on the Si-Al alloys[2] performed in our laboratory, but as one of the extensions of the previous ones with regard to the subject under consideration.

In the present investigation, the cooling curves and the micro-structures of several sand-cast specimens were preliminarily examined with regard to the normal Si-Al alloys by the ordinary metallographical methods. Essentially the same experiment was repeated in connection with those of the modified Si-Al alloys, which were prepared by adding various substances analogous to sodium in some peculiar respects. Then, the crystal structures and crystalline configurations of these two kinds of specimens, normal and modified, were examined with X-rays.

The experimental results thus obtained, were found not to be legitimately explainable by the theories of modification nowadays, as will be described below.

Specimens

In this experiment, the normal and modified Si-Al alloys of various compositions, cast at 750°C into a U-shaped sand mould (10 mm. in inner diameter and 100 mm. long), were used as the specimens. To obtain the specimens of the normal alloys, the melt was usually made to contain 7, 13 and 22 per cent. of silicon respectively, by melting the intermediate Si-Al alloy (containing about 22 per cent. of silicon)

1. e. g., H. Hirata and Y. Tanaka; These Memoirs, A, **17**, 143 (1934)
2. H. Kotô; The Anniversary Volume dedicated to Prof. Masumi Chikashige, 303 (1930)

with pure aluminium (purity 99.8 per cent.) in a morganite crucible lined with alundum cement. While, those of the modified ones were prepared by adding a small quantity of sodium or another modifier as given in the second column of Table I at 800°C, to the molten normal alloy containing 13 per cent. of silicon. The properties analogous to sodium and the other peculiarities of these modifiers are noted in the first column of the same table; whereas, the third column of Table I represents the amounts of the modifiers added to prepare the modified specimens mainly used in the present experiment. To secure unity in the experimental data obtained, all the experiments were made with the vertical portion of U-shaped ingot.

Here, it is noticed that the compositions of the specimens and the amounts of the modifiers sometimes varied from those above mentioned, according to the purposes of researches, as will be stated later.

Table I

	Modifier	Amount added (Wt.-%)	Micro-structure		Modifying Effect
			Primary Crystal	Eutectic	
Alkali Metals	Na	0.1	nil	Silumin structure	most remarkable
	Na	0.5	nil	ditto	ditto
	Na	1	very small quantity of Al crystals	ditto	somewhat inferior to the above
	Na	3	Al crystals	ditto	more inferior to the above
	Li	0.1	dendritic Al crystals	Si comes to appear in a fine grobular form	remarkable next to Na
	Li	0.5	dendritic Al crystals and large quantity of crystalline substance supposed to be of Si_2Li_6	ditto	ditto
	K	0.1	Si crystals	almost unaltered with that of the normal alloy	almost inapppreciable
	K	0.5	very small quantity of Si crystals	The central part of the ingot is composed of the eutectic containing very fine grobular grains of Si, while in the other parts, Si is crystallized in a fine needle-shape	somewhat appreciable
	K	1	ditto	Si is mostly crystallized in a fine needle-shape	rather remarkable

Table I (*Continued*)

	Modifier	Amount added (Wt.-%)	Micro-structure		Modifying Effect
			Primary Crystal	Eutectic	
Alkaline Earth Metals	Ca	0.1	The amount of the primary crystallized Si decreases in comparison with that of the normal alloy	Si comes to appear in somewhat finer needle-shaped crystals than those of the normal alloy	somewhat appreciable in part
	Ca	0.5	very small quantity of dendritic Al crystals	The eutectic being mainly composed of Si crystallized in a needle-shape of considerable dimensions, is partly of the fine structure	rather remarkable in part
	Mg	0.1	primary Si crystals surrounded by Al	The eutectic contains needle-shaped Si crystals of considerable dimensions	almost inappreciable
	Mg	0.5	very small quantity of Al crystals	The eutectic consists mainly of Si crystallized in a needle-shape	rather remarkable in part
The volatile Elements as Na	Te	0.1	Si crystals	The eutectic contains needle-shaped Si crystals	nil
	Te	0.5	ditto	ditto	ditto
	As	0.1	ditto	ditto	ditto
	As	2	The amount of the primary crystallized Si decreases in comparison with that of the normal alloy, and primary crystals of Al come to appear surrounding Si crystals	Si comes to appear in somewhat finer needle-shaped crystals than those of the normal alloy	somewhat appreciable in part
The Elements insoluble to both Al and Si as Na	Bi	0.1	Si crystals	The eutectic contains needle-shaped Si crystals	nil
	Bi	4.5	ditto	ditto	somewhat appreciable in part
	Sb	0.1	ditto	ditto	nil
	Sb	0.5	ditto	ditto	somewhat appreciable in part

In this table, the normal Si-Al alloy containing 13 per cent. of silicon is called the "normal alloy" for short.

Experimental Results

I. Micro-structure, Cooling Curve and Dilatation

The micro-photographs of some of the normal and modified specimens used in this experiment, are reproduced in Plate I. With regard to these two series of specimens, the binary constitutional diagram for the normal Si-Al alloys has already been determined by Fraenkel[1], Edwards[2] and others.[3] Moreover, despite the lack of any complete ternary constitutional diagram corresponding to the modified ones, their constitutions may also be inferred from the experimental results obtained by Mathewson,[4] Gwyer,[5] Williams[6] and Assmann[7], dealing with the binary systems as those of Na-Al, Bi-Al, Bi-Si and Li-Al respectively. It is conceivable from these diagrams that all the specimens of the normal and modified alloys under consideration are mainly composed of the eutectic, except for those of the normal ones containing respectively 7 and 22 per cent. of silicon, these two exceptions being presumed to bear the considerable amounts of the primary crystallized aluminium or silicon.[8]

As can be seen in Figs. 1, 2 and 3, Plate I, the micro-structures of the normal alloys show us, that they are composed not only of the eutectic containing needle-shaped crystals of silicon, but also of various amounts of the primary crystallized aluminium or silicon. Furthermore, the aspects of these primary crystallized substances are observed to vary with the increasing amounts of silicon contained in the specimen: i. e., in Fig. 1, Plate I, which is taken with the specimen of the normal alloy containing 7 per cent. of silicon, the primary crystals are observed to consist of the comparatively large irregular grains of aluminium;

1. Zeits. f. anorg. Chem., **58**, 154 (1908)
2. Chem. and Met. Eng., **28**, 165 (1923)
3. e. g., Roberts; J. Chem. Soc., **105**, 1383 (1914)
   Rosenhain, Archbutt and Hanson; Eleventh Report to the Alloys Research Committee of the Institution of Mechanical Engineers, (1921)
   B. Ôtani; J. Inst. Met., **36**, 243 (1926)
   A. G. C. Gwyer and H. W. L. Phillips; J. Inst. Met., **36**, 283 (1926)
4. Zeits. f. anorg. Chem., **48**, 191 (1906)
5. Zeits. f. anorg. Chem., **49**, 311 (1906)
6. Zeits. f. anorg. Chem., **55**, 1 (1907)
7. Zeits. f. Metallk. **18**, 51 (1926)
8. In this paper, aluminium containing very small amount of silicon (α-solid solution of silicon in aluminium) and silicon containing very small amount of aluminium (β-solid solution of aluminium in silicon) are respectively called "aluminium" and "silicon" for short.

while, Figs, 2 and 3, Plate I indicate that the specimens containing 13 and 22 per cent. of silicon respectively, bear the polyhedral grains of the primary crystallized silicon, and the whole amount of these primary crystals increases more markedly in the latter specimen containing 22 per cent. of silicon, than in the former one containing 13 per cent. of the same element.

From the foregoing argument advanced in connection with the normal alloys, it became clear that their micro-structures coincide fairly well with the constitutional diagram of Si-Al system. Not only these, but the micro-structures of the modified alloys, which were partly reproduced in the figures following Fig. 4, Plate I, and tabulated in the third column of Table I, also indicate the predomination of the eutectic, as was previously inferred from the constitutional diagrams. Consequently, we may conclude that all the specimens of the normal and modified alloys examined are of usual micro-structure.

If we inspect the micro-photographs of the modified specimens in Plate I more minutely, the modifying effect of adding each element can easily be detected from the refinement of their micro-structures. The effect thus confirmed is shown in the fourth column of Table I.

In this table, not only sodium but the other alkali metals examined, such as lithium and potassium, are also found to be very efficacious for the modification of Si-Al alloy. Furthermore, it is seen that calcium and magnesium, belonging to the alkaline earth metals, come the next to these alkali metals in the conspicuousness of their modifying effect.

Contrary to the elements above mentioned, phosphorous, sulphur, selenium, tellurium and arsenic, which bear resemblance to sodium in their volatility, give rise to so slight a modification generally as to be hardly appreciable. Even in the special cases when these volatile elements were found somewhat efficacious for the modification, the aspects of the modifying effect considerably differed from that caused by sodium : e. g., the modifying effect of tellurium could only be detectable with the addition of the comparatively larger amount (about 5 per cent.), than those added in the cases of the alkali or alkaline earth metals. These facts above confirmed, can hardly be explainable by attributing the modifying agent of sodium to its volatility.

The modifying effects of adding bismuth and antimony, which are miscible neither to aluminium nor silicon, were also examined microscopically and tabulated again in the fourth column of Table I. As can be seen in this table, these two elements were also confirmed

not to be efficacious for the modification, as the volatile ones. Moreover, with regard to the modifying effects of some other elements belonging to this category, such as lead, cadmium and thallium, the same examination was carried out, but no sign of the modification could be observed even in these cases. Thus, the ternary constituents theory, which attributes the modifying agent of sodium to its separation from the molten Si-Al alloys by cooling, may hardly be said to explain the mechanism of modification at large.

To make the further confirmation on the mechanism of modification of Si-Al alloys, the thermal analysis was made in connection with the normal and modified alloys both containing less than 16 per cent. of silicon. Some of the cooling curves thus obtained are reproduced in Fig. 16.

As can be seen in Fig. 16, the results of the thermal analysis above stated were found to be essentially the same as those given by B. Ôtani,[1] who disproved the under-cooling theory of modification of

Fig. 16

Cooling Curves of Normal and Modified Alloys.

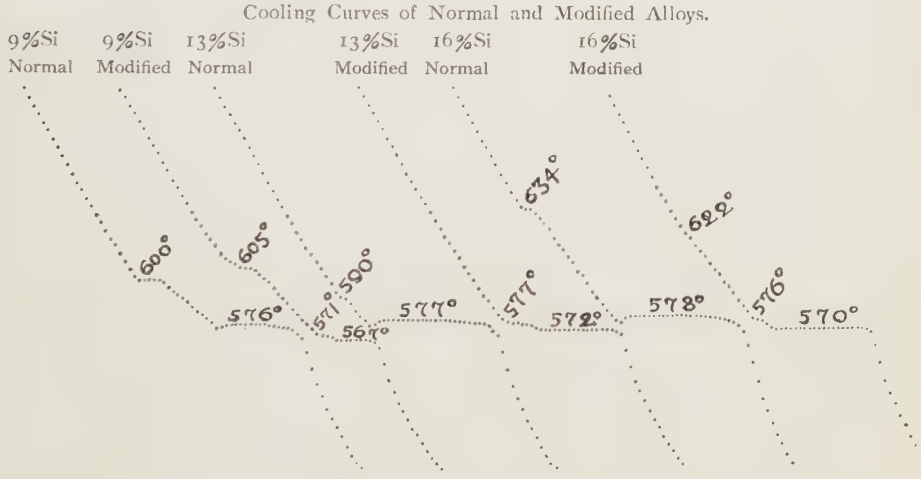

Si-Al alloys: i. e., the fair agreements between the cooling curves obtained by both series of examinations can be observed, not only with respect to the fact that the temperature of primary crystallization of the alloy modified with sodium is higher than that of the corresponding normal alloys in the aluminium side, but with regard to many other points. Especially, it is noticed that the curves obtained in connection

1. Loc. cit.

with the normal alloys in Fig. 16, similarly as those given by B. Ôtani, have the more remarkable indentations indicating the under-cooling of the specimens at the temperatures of primary and eutectic crystallization, than the curves corresponding to the modified ones containing a small quantity of sodium. Thus, the under-cooling theory of modification of Si-Al alloys, as well as the considerations based upon the volatility of sodium or the formation of ternary constituents before mentioned, seems to be exceptional, if not unreasonable, in this respect.

Here, it may be advisable to append the results of our examination on the abnormal dilatations of various specimens, which was carried out by means of the improved differential self-photographing dilatometer.[1] Some of the dilatation curves thus obtained by making use of pure aluminium as the standard, are shown in the annexed figure, Fig. 17.

Among these curves in Fig. 17, that represented by A was taken with the sand-cast specimen of the normal alloy left as it is. From this curve, the specimen above mentioned is seen to expand abnormally at about 350°C on heating. But, such an abnormal dilatation could no more be detectable from the curve represented by B, which was taken with the specimen once used in the former examination. These facts above mentioned show us without doubt, that the abnormal dilatation above stated is of the irreversible variety.

The dilatation curves following C in Fig. 17 were similarly taken as the curve A in the same figure, with some of the sand-cast specimens of the modified alloys. As may be seen in these curves, the abnormal dilatation observed with the specimen of the normal alloy can also be detected even with those of the modified ones containing the third elements. But, it is noticed that this abnormal dilatation came to appear the less markedly in the curves taken with the specimens of the more modified structure, as was observed with some of the specimens containing the alkali or alkaline earth metals.

1. D. Uno, S. Yoshida and S. Katori ; A Report of the Institute for Chemical Research, Imperial University, Kyoto, **3**, 152 (1933)

Fig. 17 a

The Differential Dilatation Curves of the Normal and Modified Alloys containing 13 per cent. of silicon.

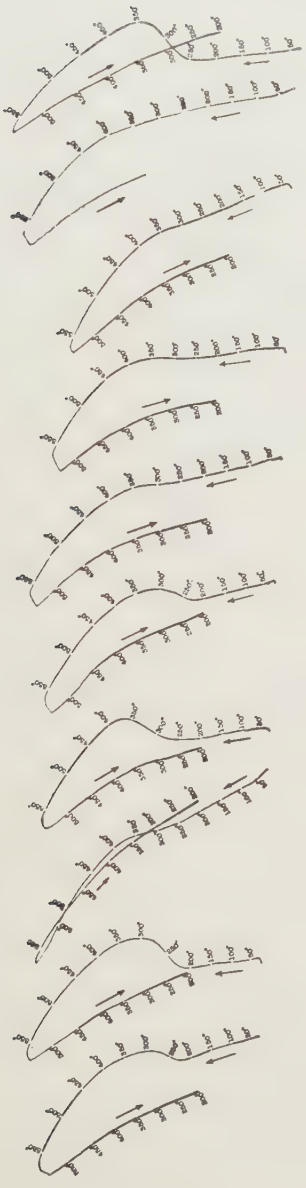

A. The sand-cast specimen of the normal alloy left as it is.

B. The specimen once used in the former examination.

C. Modified alloy containing 0.1%Na.

D. Modified alloy containing 1%Na.

E. Modified alloy containing 0.1%Li.

F. Modified alloy containing 0.5%Li.

G. Modified alloy containing 0.1%K.

H. Modified alloy containing 0.5%K.

I. Modified alloy containing 0.1%Mg.

J. Modified alloy containing 0.5%Mg.

Fig. 17 b

The Differential Dilatation Curves of the Normal and Modified Alloys containing 13 per cent. of silicon.

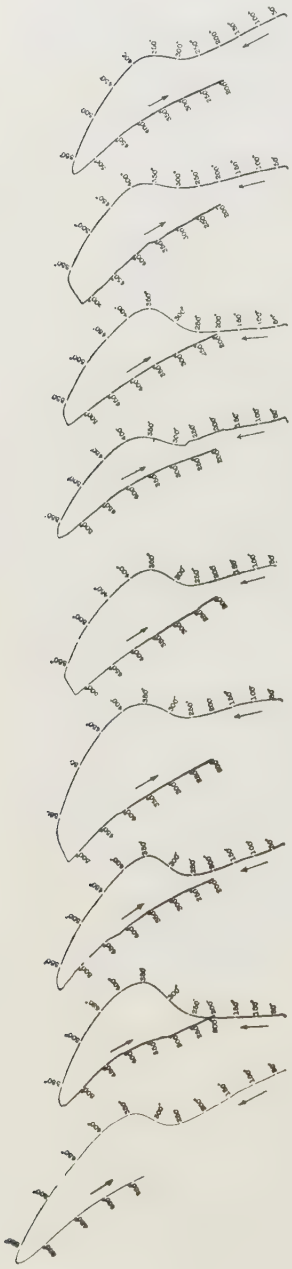

K. Modified alloy containing 0.1%Ca.

L. Modified alloy containing 0.5%Ca.

M. Modified alloy containing 0.1%Bi.

N. Modified alloy containing 4.5%Bi.

O. Modified alloy containing 0.1%Sb.

P. Modified alloy containing 0.5%Sb.

Q. Modified alloy containing 0.1%Te.

R. Modified alloy containing 0.1%As.

S. Modified alloy containing 2%As.

II. Crystalline Configuration

X-ray examination was first carried out by means of Laue's method, as was the case with Shinoda[1], to see whether or not the micro-structure of the specimens above mentioned gives any accurate information in connection with the actual size and configuration of the micro-crystals. In this research, only the Si-Al alloys of the normal form of various compositions, and those modified by adding a small quantity of sodium, lithium, and bismuth respectively, were used as the specimens. To utilize the specimens in this examination, two series of thin plates (about 3 mm. in thickness) were respectively cut out from the vertical portion of each ingot, parallel and perpendicularly to its longitudinal axis and polished until they were reduced to about 1 mm. in thickness. When the planed surface of the specimens was set perpendicularly to the incident X-ray beam, two series of the diffraction patterns could be obtained; the one is given rise by the incidence of X-rays parallel to the longitudinal axis of ingot (named longitudinal incidence for convenience sake), while the other corresponds to the normal incidence (named transversal incidence).

Some of the diffraction patterns thus obtained are reproduced in Plates II and III. It is noticed that not only those here reproduced, but all the patterns due respectively to the longitudinal and transversal incidences of X-rays to the same specimen, were also found not essentially different to each other.

As can be seen in Figs. 18 and 19, Plate II, both diffraction patterns produced by the transversal and longitudinal incidences of X-rays to the normal alloy containing 7 per cent. of silicon, consist of an irregular assemblage of somewhat elongated Laue's spots. Thus, we may conclude from the presence of elongated Laue's spots in both figures above mentioned, that the specimen under examination is composed of crystals of comparatively large size, and bears a fibrous nature of weak degree.

Figs. 20 and 21, Plate II are the diffraction patterns taken with the alloy containing 13 per cent. of silicon in a similar way as Figs. 18 and 19, Plate II. The prominent parts of these patterns consist of several long radiating bands and a number of Debye-Hull's rings. Thus, it can be concluded from the presence of radiating bands in Figs. 20 and 21, Plate II, that the specimen under consideration is

1. Loc. cit.

partly composed of a fibrous structure: But, the presence of Debye-Hull's rings shows us that the considerable portion of it consists of an irregular aggregation of the micro-crystals smaller than those in the former specimen containing 7 per cent. of silicon. By the aid of an improved Yoshida's crystallographic globe,[1] the axis of the fibre in this case was found to coincide with the normal to one of the icositetrahedral faces (211) of the cubic crystal. While, Debye-Hull's rings in the same figures were confirmed to be due to the molybdenum K_α radiation reflected from the prominent atomic planes $(111)_1$, $(100)_1$, $(110)_1$, $(113)_1$, $(111)_2$, $(100)_2$, $(133)_1$ and $(120)_1$ of the aluminium crystal. Here it must be understood that the numerical suffixes used in the symbols $(\quad)_1$ and $(\quad)_2$, denote the order of the spectrum.

In short, the specimen containing 13 per cent. of silicon may be said to be made up by the more irregular arrangement of the micro-crystals, which are of the smaller dimension than those of the specimen containing 7 per cent. of silicon.

Such a violation of the regularity of the crystalline configuration due to the increasing amount of silicon, was observed more markedly in the specimen containing 22 per cent. of silicon. The diffraction patterns occurring from this specimen are reproduced in Figs. 22 and 23, Plate II. As is seen in these figures, both diffraction patterns corresponding to the transversal and longitudinal incidences of X-rays, consist mainly of a number of Debye-Hull's rings, which were conceived to be due to the same atomic planes of aluminium, as in Figs. 20 and 21, Plate II. The predomination of such Debye-Hull's rings in Figs. 22 and 23, shows us without doubt that this specimen is nothing but an aggregation of the finer micro-crystals without any regularity.

From the foregoing argument in connection with the normal alloys, we may conclude that the smaller amount of silicon contained in the specimen, the more favourable were the conditions for the formation of large crystals and regular structures, at least within the scope of our investigation. The above conclusion does not agree so well with the results of the microscopical examinations, according to which the size of crystallites, as can be seen in Figs. 1, 2 and 3, Plate I, remains nearly unaltered by the increasing amount of silicon contained in the specimen.

1. U. Yoshida; Japanese J. Phys., 133 (1927), and S. Takeyama; These Mem irs, A, **11**, 467 (1928)

Such a discrepancy of the crystalline configuration to the micro-structure, could be observed more markedly by taking into account the diffraction phenomena due to the modified specimens. As the case in point, we may refer to the diffraction patterns in Figs. 24, 25, 26, Plate II and Fig. 27, Plate III, which were given rise by the specimens modified with a small quantity of sodium. The diffraction patterns above mentioned consist mainly of a set of short radiating bands[1] or somewhat elongated Laue's spots, associated with several Debye-Hull's rings: While, in the patterns taken with some of the specimens of the normal alloys, nothing but Debye-Hull's rings could previously be detected, as was the case with the specimen containing 22 per cent. of silicon (see Figs. 22 and 23, Plate II). Thus, it may be said that the crystalline configuration is more regulated in these modified specimens than in some of the normal alloys. Furthermore, contrary to the results of the microscopical examination, the predomination of Laue's spots in Fig. 26, Plate II and Fig. 27, Plate III, instead of Debye-Hull's rings in Figs. 22 and 23, Plate II, shows us that the crystallites constituting the modified specimens with 3 per cent. of sodium, are at least of the larger dimension than those of the normal alloy containing 22 per cent. of silicon.

Not only with the specimens above mentioned, but with some other specimens, the same inconsistency of the diffraction pattern to the micro-structure was also observed; e. g., such an inconsistency can easily be seen by comparing Figs. 28 and 30, Plate III, or Fig. 26, Plate II and Fig. 34, Plate III. Thus, we may conclude that the micro-structure of Si-Al alloys informs us very little with regard to the actual crystalline configuration.

In our foregoing consideration, there remains still doubtful, if the procedure of cutting and polishing the specimens would inflict too much mechanical distortions upon the crystalline configuration of their surfaces, to give rise to any reliable diffraction figure. By way of removing the effect of such an infliction, the writer once tried to etch off the outer portion of each specimen by pickling it in the mixture of hydrochloric and hydrofluoric acid, before the X-ray examination. But, owing to the unequal corrosion of the constituents of the specimens, it was found impossible to do so without changing their composition. Therefore,

1. The angular distribution of these radiating bands can also be realized by the rotation of a cubic crystal within a certain angle, around the normal direction to one of its (211) planes.

the writer was obliged to estimate the effect under consideration by comparing the diffraction patterns taken with two kinds of the specimens of pure aluminium: The one was prepared in the similar way as the specimens of Si-Al alloy examined, while to obtain the other, the specimen of pure aluminium thus prepared was pickled in hydrochloric acid. As the consequence of this estimation, it was confirmed that the diffraction patterns given rise by these two kinds of specimens were essentially the same. This shows us that even in such a comparatively soft metal as pure aluminium, the effect of the mechanical distortion is very slight; still less it should be the case with the comparatively hard alloys as were used in the present research.

III. Crystal Structure

Despite the remarkable difference in their constitutional diagrams with aluminium and silicon, the alkali metals such as sodium and lithium were microscopically found to bear resemblance in their conspicuous modifying effects on the structure of Si-Al alloys, as stated before. In this respect, the more accurate confirmation with regard to the relation between the constitutional diagrams and the modifying effects, seems to be needed for a further consideration. Therefore, the writer repeated the X-ray examination, to make clear the crystal structure of Si-Al alloys corresponding to some of the phases in the constitutional diagrams.

In this experiment, not only the specimens of the normal form, but those modified by adding sodium and lithium respectively, were also examined after the ordinary powder method, with a quadrant spectrograph of 7.5 cm. in radius. Each one of these specimens was pulverised and then was sealed in a small glass tube to be mounted in the spectrograph. When the powdery crystals thus prepared were illuminated by the incident X-ray beam, the spectra of the molybdenum K characteristic radiation usually came to appear as shown in the figures of Plate IV. By measuring the distances of these spectral lines from the central one, we obtain the numerical values shown in Table II.

As can be seen in Figs. 37, 38 and 39, Plate IV, all the spectra of the normal alloys, were confirmed to be nothing but the superposition of two series of the spectral lines, each one of which was reflected respectively from the prominent atomic planes of the powdery crystals of aluminium and silicon. The increasing amount of silicon

Table II

Indices of Al		$(111)_{1\beta}$	$(111)_{1\alpha}$	$(100)_{1\alpha}$		new line		$(110)_{1\beta}$	$(110)_{1\alpha}$		$(113)_{1\beta}$	new line		$(113)_{1\alpha}$	$(111)_{2\alpha}$		new line	new line		$(133)_{1\beta}$	$(100)_{2\alpha}$	$(133)_{2}$	$(200)_{2}$	$(211)_{2}$	$(111)_{3}$
Pure Al		2.03	2.29	2.64				3.36	3.77		3.99			4.44	4.67					5.24	5.41				
7% Si alloy	1.70	2.00	2.29	2.65				3.35	3.76		3.95			4.44	4.66	4.93					5.37				
13% Si alloy	1.70	2.03	2.28	2.65	2.84			3.32	3.78		3.98			4.46	4.68	4.93			5.22		5.40				
22% Si alloy	1.70	2.05	2.29	2.63	2.81			3.29	3.75		3.95			4.42	4.61	4.87			5.16		5.34				
Al alloy containing 5% Na		2.02	2.28	2.64				3.35	3.78		3.95			4.45	4.66						5.40				
Al alloy containing 20.4% Na		2.03	2.30	2.67				3.37	3.79		3.98			4.47	4.68						5.40				
Modified alloy containing 0.1% Na	1.70	2.03	2.28	2.64	2.80			3.29	3.76		3.95			4.43	4.65	4.90			5.20		5.37				
Modified alloy containing 3% Na	1.72	2.04	2.30	2.65	2.84			3.30	3.79		3.97			4.45	4.65	4.93			5.21		5.39				
Modified alloy containing 5% Na	1.70	2.01	2.29	2.65	2.81			3.32	3.77		3.97			4.45	4.66	4.91			5.22		5.40				
Modified alloy containing 20.4% Na		2.03	2.28	2.64				3.34	3.79					4.47	4.68						5.41				
Al alloy containing 2% Li		2.06	2.30	2.68				3.38	3.82		4.02			4.48	4.74						5.43				
Al alloy containing 7% Li		2.05	2.29	2.65				3.37	3.77		3.99			4.45	4.69						5.41				
Al alloy containing 17% Li		2.11	2.41	2.71		2.87		3.43	3.81			4.26		4.53			4.92	5.15			5.53				
Al alloy containing 20.4% Li			2.35	2.67		2.84		3.41	3.78			4.23		4.48	4.68						5.49				
Modified alloy containing 0.1% Li	1.71	2.03	2.28	2.62	2.81			3 30	3.75		3.95			4.40	4.63	4.93			5.19		5.35				
Modified alloy containing 0.5% Li	1.71	2.02	2.30	2.66	2.85			3.32	3.79		3.99			4.44	4.66	4.91			5.21		5.40				
Modified alloy containing 2% Li	1.71	2.03	2.28	2.63	2.84			3.31	3.78		3.98			4.42	4.65	4.92			5.20		5.40				
Modified alloy containing 17% Li			2.30	2.60				3.38	3.77			4.18		4.43							5.41				
Modified alloy containing 20.4% Li			2.35	2.68				3.40	3.79		4.00	4.21		4.48	4.70		4.85	5.10							
Pure Si	1.71				2.80		3.28			3.96			4.34			4.92			5.21			5.64		5.95		6.80	
Indices of Si	$(111)_1$				$(110)_2$		$(113)_1$			$(100)_4$			$(133)_1$			$(211)_2$			$(115)_1$ $(111)_3$			$(110)_4$		$(135)_1$		$(130)_2$	

contained in the specimens from 7 and 13 per cent. to 22 per cent., only intensifies the series of lines corresponding to the silicon crystals, but does not affect the position of any line in these spectra. Such an unalteration of the spectral lines indicates that the solubility between aluminium and silicon is extremely small. Consequently, this confirms the binary constitutional diagram of the Si-Al system previously determined, to be correct.

The spectral lines of the specimens of Si-Al alloys modified with various quantities of sodium, are reproduced in Figs. 42, 43, 44 and 45, Plate IV. For the convenience of comparison, similar examinations were also carried out with the specimens of aluminium containing the same amounts of sodium as above. Some of the spectral lines thus obtained with these specimens are shown in Figs. 40 and 41, Plate IV.

In two series of figures here reproduced, the unalteration of the positions of spectral lines irrespective to the composition, which has already been observed with the normal alloys, may also be found to hold even with regard to these specimens containing some sodium. Thus, we may conclude that not only aluminium and silicon are hardly soluble in the solid state to each other, but sodium is also insoluble to these two elements, as was suggested by the constitutional diagrams.

Nevertheless, this unalteration is violated in the case when lithium, instead of sodium, was added to the specimens: i. e., as can be seen in the spectra reproduced from Fig. 46 to Fig. 54, Plate IV, the deviation of the lines corresponding to aluminium and silicon, became markedly observable with the increasing amount of lithium. Furthermore, some new lines supposed to be caused by the compound of aluminium and lithium, appeared in the spectra of the specimens containing comparatively large amount of lithium. These facts indicate that the transformation of space lattices in the specimens took place with the addition of lithium.

The consideration confirmed above with regard to the specimens containing lithium agrees well with the binary constitutional diagrams of the Li-Al and Li-Si systems, according to which not only the solid solution extending to the comparatively wide scope in composition, but the intermetallic compounds between lithium and aluminium or lithium and silicon, such as Al Li or Li_6Si_2, should exist. Thus, notwithstanding the similarity in the modifying effects of sodium and lithium on Si-Al alloy as stated before, these two modifiers may be said to be entirely

different in their alloying properties to each component of Si-Al alloy. This confirms again our foregoing opposition to the theory of modification based upon the formation of ternary constituents.

Summary

The experimental results which have hitherto been described in connection with the sand-cast specimens of various normal and modified Si-Al alloys, lead us to the following conclusions :—

(a) The crystal structure of these specimens as well as their micro-structure is in good accordance with the corresponding constitutional diagrams.

(b) The elements efficacious for modifying the specimens are not necessarily either volatile or immiscible to aluminium and silicon, as was suggested by the present theories of modification : But, they should partake of the chemical properties analogous to sodium.

(c) The cooling curves show us that the specimens of the normal alloys have undergone the more remarkable under-cooling phenomena than those of the modified ones containing a small quantity of sodium.

(d) There are some discrepancies between the actual crystalline configuration in the specimens and their micro-structure.

Among these four propositions (a), (b), (c) and (d), which were deduced as the necessary consequences of our experimental results, (b) could hardly be explained by attributing the modifying agents of the modifiers to their volatility. Also, from (a) and (b), some elements of the appreciable solubility to both aluminium and silicon, such as lithium, were found to be also efficacious for the modification of Si-Al alloy. Thus, Ôtani's[1] ternary constituents theory and Gwyer's[2] protective colloid theory, which attribute the conspicuous modifying agent of sodium to its small miscibility to both aluminium and silicon, may be said not to be applicable at least in the case of lithium. But, it is here noticed that the modifying agents of these two elements, sodium and lithium, to Si-Al alloy, are too similar to be conceived of as different mechanisms. Moreover, the proposition (c) was not in good accordance with the under-cooling theory of modification. In short, the foregoing propositions (a), (b) and (c) could hardly be explained by the theories of modification nowadays, without some special assump-

1. Loc. cit.
2. Loc. cit.

tions. Not only these, but the proposition (d) showed us the necessity of further considerations before the mechanism of modification of Si-Al alloys is described in terms of the space-lattice theory on crystallography.

Contrary to the above, the elements belonging to the alkali and alkaline earth groups were found to partake remarkably of the modifying agent, as was pointed out by the proposition (b). This fact seems to suggest the concealment of some "atomistic", instead of "thermodynamical", causes giving rise to the modification of Si-Al alloy.

In conclusion, the writer wishes to express his thanks to Prof. D. Uno and Dr. H. Hirata for their kind guidance and invaluable advice. His thanks are also due to the Imperial Academy of Japan for the fund granted for the present investigations.

Institute of Metallography,
Kyoto Imperial University.

Plate I

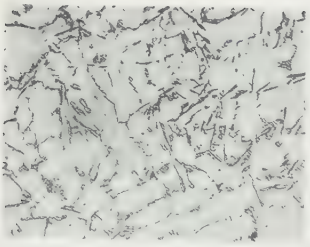

Fig. 1.—7% Si. ×100

Fig. 2.—13% Si. ×100

Fig. 3.—22% Si. ×100

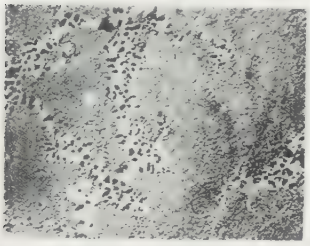

Fig. 4.—Modified with 0.1% Na. ×100

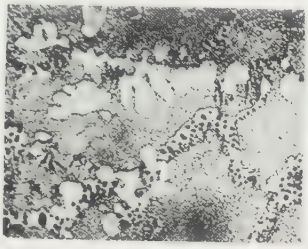

Fig. 5.—Modified with 3% Na. ×100

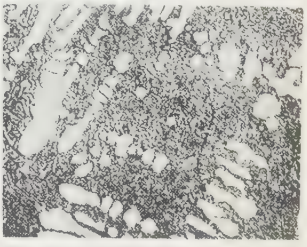

Fig. 6.—Modified with 0.1% Li. ×100

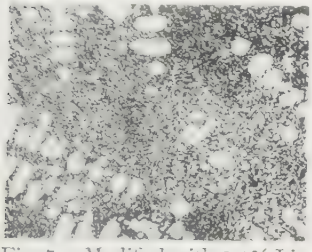

Fig. 7.—Modified with 0.5% Li. ×100

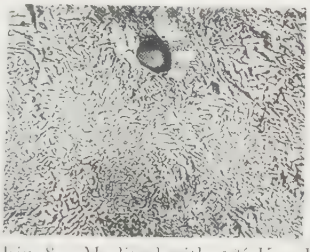

Fig. 8.—Modified with 1% K. ×100

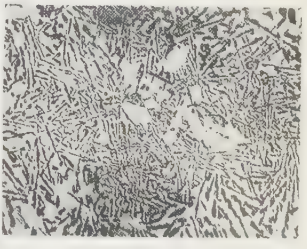

Fig. 9. Modified with 0.5% Mg. ×100

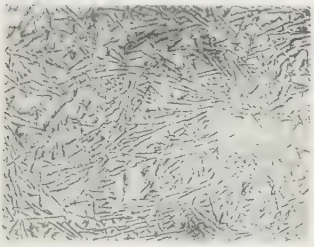

Fig. 10. Modified with 0.5% Ca. ×100

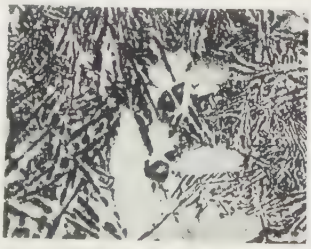

Fig. 11. Modified with 2% As. ×100

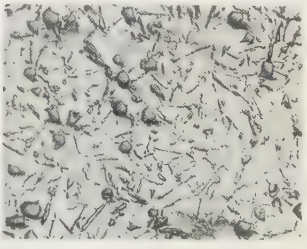

Fig. 12.—Modified with 0.5% Te. ×100

Fig. 13.—Modified with 0.1% Bi. ×100

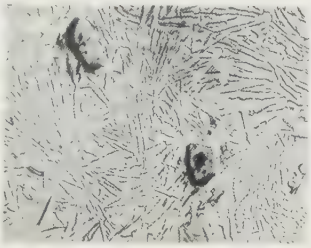

Fig. 14. Modified with 1.5% Bi. ×100

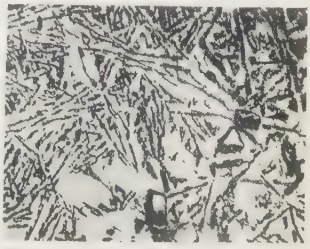

Fig. 15. Modified with 0.5% Sb. ×100

Plate II

Fig. 18.—7% Si.
Transversal Incidence.

Fig. 19.—7% Si.
Longitudinal Incidence.

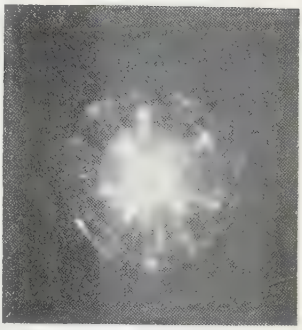

Fig. 20.—13% Si.
Transversal Incidence.

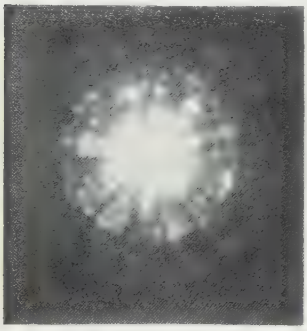

Fig. 21.—13% Si.
Longitudinal Incidence.

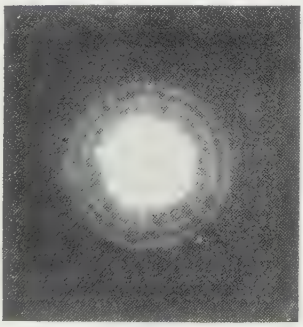

Fig. 22.—22% Si.
Transversal Incidence.

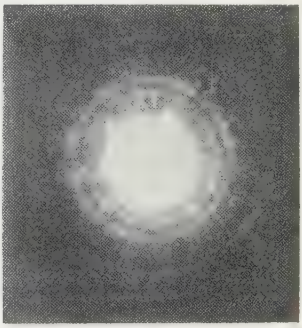

Fig. 23.—22% Si.
Longitudinal Incidence.

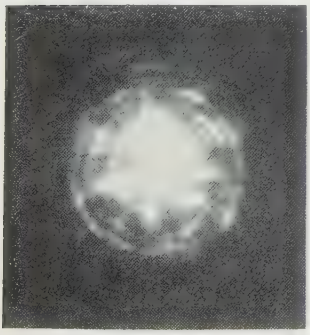

Fig. 24.—Modified with 0.1% Na.
Transversal Incidence.

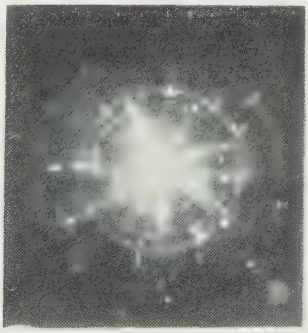

Fig. 25.—Modified with 0.1% Na.
Longitudinal Incidence.

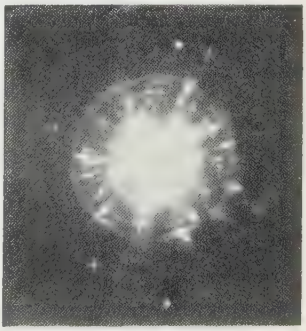

Fig. 26.—Modified with 3% Na.
Transversal Incidence.

Plate III

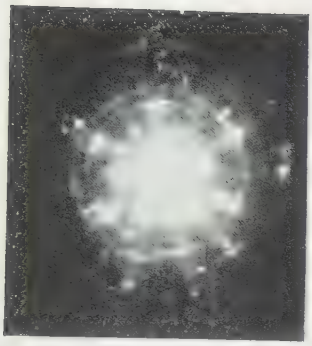

Fig. 27.—Modified with 3% Na.
Longitudinal Incidence.

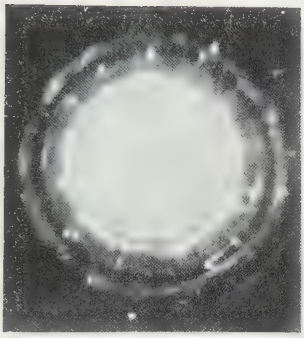

Fig. 28.—Modified with 0.1% Li.
Transversal Incidence.

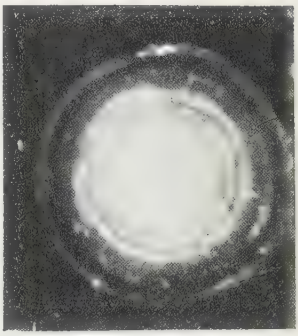

Fig. 29.—Modified with 0.1% Li.
Longitudinal Incidence.

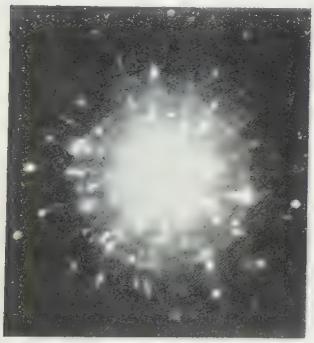

Fig. 30.—Modified with 0.5% Li.
Transversal Incidence.

Fig. 31.—Modified with 0.5% Li.
Longitudinal Incidence.

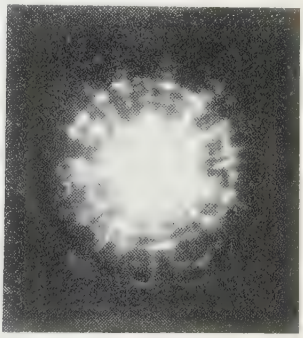

Fig. 32.—Modified with 0.1% Bi.
Transversal Incidence.

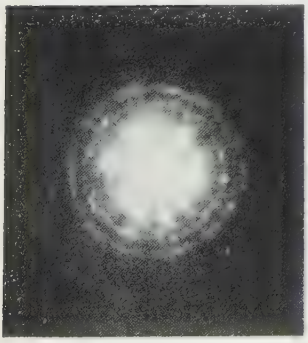

Fig. 33.—Modified with 0.1% Bi.
Longitudinal Incidence.

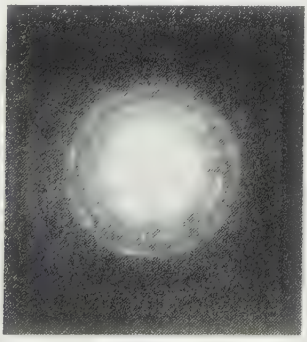

Fig. 34.—Modified with 4.5% Bi.
Transversal Incidence.

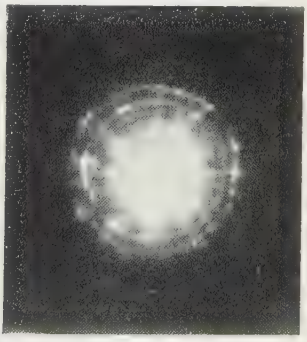

Fig. 35.—Modified with 4.5% Bi.
Longitudinal Incidence.

Plate IV

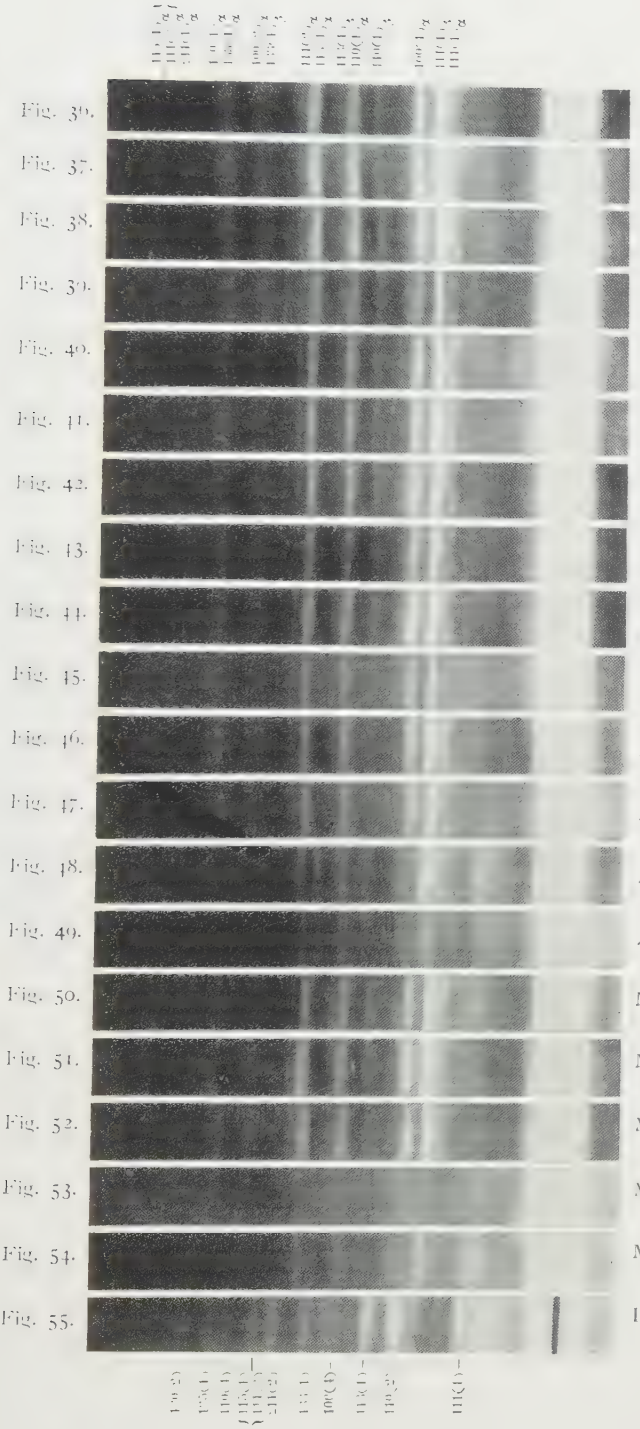

Fig. 36. Pure Al
Fig. 37. 7% Si alloy
Fig. 38. 13% Si alloy
Fig. 39. 22% Si alloy
Fig. 40. Al alloy containing 5% Na
Fig. 41. Al alloy containing 20.4% Na
Fig. 42. Modified alloy containing 0.1% Na
Fig. 43. Modified alloy containing 3% Na
Fig. 44. Modified alloy containing 5% Na
Fig. 45. Modified alloy containing 20.4% Na
Fig. 46. Al alloy containing 2% Li
Fig. 47. Al alloy containing 7% Li
Fig. 48. Al alloy containing 17% Li
Fig. 49. Al alloy containing 20.4% Li
Fig. 50. Modified alloy containing 0.1% Li
Fig. 51. Modified alloy containing 0.5% Li
Fig. 52. Modified alloy containing 2% Li
Fig. 53. Modified alloy containing 17% Li
Fig. 54. Modified alloy containing 20.4% Li
Fig. 55. Pure Si

An Integral Equation with a Parameter

By

Tunezô Satô

(Received November 26, 1934)

Mr. A. Kawaguchi derived the integral equation

$$(1) \qquad \varphi(x)=\lambda A(x)\varphi(x)+\lambda\int_a^b K(x, y)\varphi(y)dy,$$

where $K(x, y)$ being finite and continuous in the square-domain D $a\leqq x\leqq b$, $a\leqq y\leqq b$, moreover real and symmetric; λ being a parameter $[|\lambda|<+\infty]$.

In this paper, I will prove the following

Theorem. *When $A(x)$ has the same sign throughout the interval and $|A(x)|$ always small values, there exists at least a solution, which does not vanish identically, of the integral equation*

$$\varphi(x)=\lambda A(x)\varphi(x)+\lambda\int_a^b K(x, y)\varphi(y)dy.$$

For the purpose of simplifying the demonstration, we denote Fredholm's determinant of $A(x, y)$ by

$$D[A]=1+\sum_{n=1}^{\infty}\frac{(-1)^n}{n!}\int_a^b\cdots\int_a^b A\begin{pmatrix}z_1, z_2, \ldots\ldots, z_n\\ z_1, z_2, \ldots\ldots, z_n\end{pmatrix}dz_1dz_2\ldots\ldots dz_n.$$

Let

$$(2) \qquad L(x, y;\ \lambda)=\frac{\lambda K(x, y)}{1-\lambda A(x)},$$

then the integral equation (1) will take the form

$$(3) \qquad \varphi(x)=\lambda\int_a^b L(x, y;\ \lambda)\,\varphi(y)dy,$$

therefore our problem is reduced to the investigation about zeros of

1. It is usual to be denoted by D_A.

Fredholm's determinant $D[\lambda K]$ i. e. $D\begin{bmatrix} \lambda K(x, y) \\ 1-\lambda A(x) \end{bmatrix}$. In order that the integral or some iterated integral of $L(x, y; \lambda)$ in D for any λ may exist, the set of λ which satisfies the equation $1-\lambda A(x)=0$ for any x must be excluded from the all λ-plane.

Now suppose $A(x)>0$ for any x. From giving such a number $\delta>0$ independent on x and λ that $1-\lambda A(x_0)=w$, $|w|\geqq\delta$ for $x=x_0$, we consider their correspondence (circle-circle) between w- and λ-plane. Then a general state of these results will appear as Fig. 1 in which dashes show each pair of corresponding points.

Fig. 1

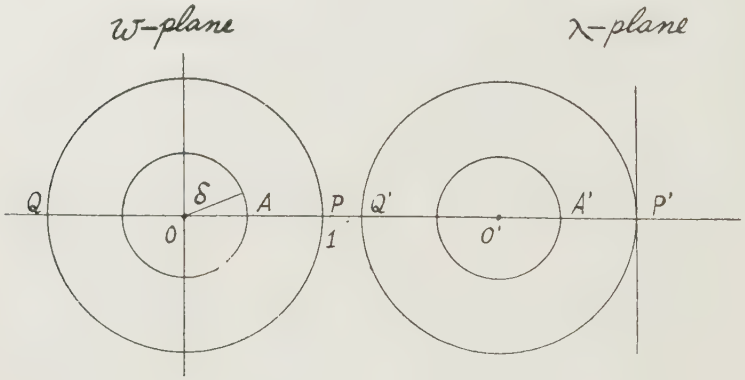

$$\left.\begin{aligned} &OA=\delta, \\ &O'A'=\delta/A_0, \\ &OP=1, \\ &O'P'=1/A_0, \\ &OQ=1, \\ &O'Q'=2/A_0, \\ &A(x_0)=A_0. \end{aligned}\right\}$$

Now when we denote the closed domain bounded by a circle with its radius δ/A_0, having the point O' as its center by $\Omega(x_0)$, and the compliment $\Omega'(x_0)$ in the λ-plane, then the function $L(x_0, y; \lambda)$ will be regular with respect to λ for any value of y. As the point x_0 moves throughout the interval (a, b), a certain domain will be swept by the circular domain $\Omega(x_0)$; say E, then $\Omega(x)<E$ for all values of x. Let

$$\beta\geqq A(x)\geqq\alpha>0,$$

then evidently

$$\frac{\delta}{\beta} \leqq \frac{\delta}{A(x)} \leqq \frac{1}{\alpha}, \quad \frac{1}{\beta} \leqq \frac{1}{A(x)} \equiv O'P' \leqq \frac{1}{\alpha}, \quad \text{and}$$

$$\frac{2}{\beta} \leqq \frac{2}{A(x)} \equiv P'Q' \leqq \frac{2}{\alpha}$$

$$\begin{cases} XP' = \dfrac{1}{\beta}, \\ YP' = \dfrac{1}{\alpha}. \end{cases}$$

Fig. 2

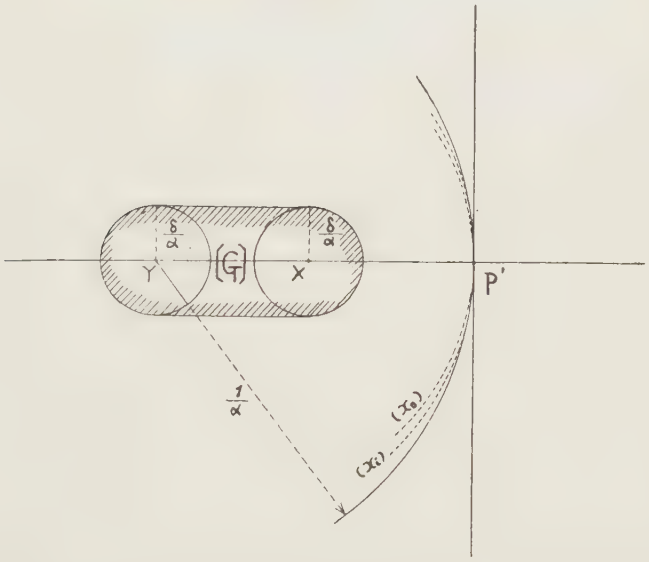

Next when we denote the domain swept by the circular domain with the radius δ/α, as the center goes from Y to X, by G, then we have $E \leqq G$.

Thus for any point (x, y) in D the function $L(x, y; \lambda)$ becomes regular with respect to λ everywhere in the compliment G' of G. Let $L_n(x, y; \lambda)$ be the n-th iterated kernel of $L(x, y; \lambda)$, and $l(x, y; \lambda, \mu)$ the reciprocal kernel; namely

$$l(x, y; \lambda, \mu) = -\sum_{h=0}^{\infty} \mu^h L_{h+1}(x, y; \lambda).$$

In view of the construction of these iterated kernels, it is clear that $L_{h+1}(x, y; \lambda)$ will be a regular function of λ in G' for any point (x, y)

in D, therefore $l(x, y; \lambda, \mu)$ will also be a regular function of λ for any point (x, y) in D and within the convergence-circle of μ.

Now for a provisional fixed value of λ in G', we have

$$\frac{\frac{d}{d\mu}D[\mu L]}{D[\mu L]} = -\sum_{h=0}^{\infty}\mu^h l_{h+1}(\lambda)$$

$$l_{h+1}(\lambda)=\int_a^b L_{h+1}(x, x; \lambda)dx,$$

where $D[\mu L]$ expresses a transcendental integral function of μ for a provisional fixed point λ in G', and at the same time a regular function of λ for a provisional fixed point μ.

Thus we can prove that *the kernel* $L(x, y; \lambda)$ *has at least one characteristic constant in the neighbourhood of* $\lambda=0$. In other words it is sufficient for us that the spur $l_1(\lambda)$ does not vanish in the neighbourhood of $\lambda=0$. Since

$$l_1(\lambda)=\iiiint L(x, u; \lambda)L(u, t; \lambda)L(t, v; \lambda)L(v, x; \lambda)du\,dv\,dt\,dx$$

and $L(x, y; \lambda)$ is regular with respect to λ in G', on account of (2),

$$l_1(0)=\iiiint K(x, u)\,K(u, t)\,K(t, v)\,K(v, x)\,du\,dv\,dt\,dx$$

$$=\iint[K_2(x, t)]^2 dt\,dx.$$

Therefore $l_1(0)\geqq 0$. Now if $l_1(0)=0$, then for any x and t

$$0=K_2(x, t)=\int_a^b K(x, u)\,K(u, t)du\,;\ \text{accordingly}$$

$$0=\int_a^b[K(x, u)]^2 du.$$

Hence we have $K(x, u)\equiv 0$ for any x and u. This is absurd.

Consequently we can conclude that for any value of λ within a circle C, having the point $\lambda=0$ as its center, there exists always the zero $\mu(\lambda)$ which satisfies the equation $D[\mu L]=0$. Especially when we take the one with the least modulus as $\mu(\lambda)$, the function $\mu(\lambda)$ is finite and regular in C from the above stated properties of $D[\mu L]$; namely the existence-domain of $\mu(\lambda)$ is the circular domain which is bounded by C. Since $\mu(0)$ is evidently a characteristic constant of the symmetric kernel $K(x, y)$, it is a real number.

Now let g be a certain real number, which $|g|$ may be taken so great that

$$|g\lambda|\geqq|\mu(\lambda)| \quad \text{on } C.$$

Fig. 3

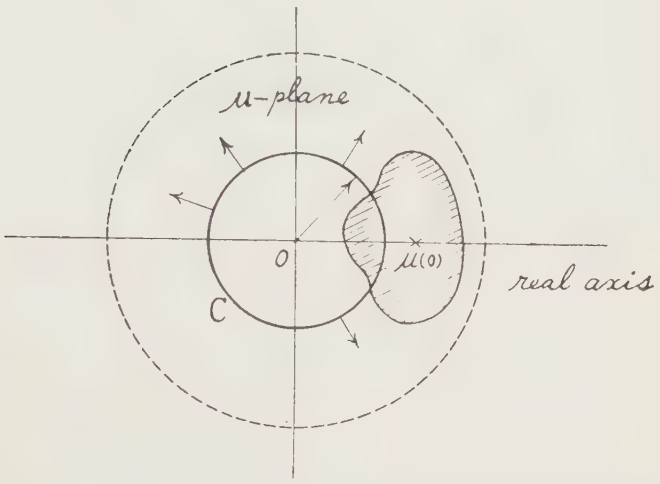

Thus when we consider a new kernel $\frac{1}{g}K(x, y)$ instead of $K(x, y)$, we see at once that there will exist a corresponding characteristic constant $\mu_1(\lambda)$ to $\mu(\lambda)$, and evidently $\mu_1(\lambda)=\frac{1}{g}\mu(\lambda)$. Hence we have $|\lambda| \geqq |\mu_1(\lambda)|$ on C.

On the other hand, let β be so small sufficiently that the domain G will be pushed out of the circle C, then the above stated circular domain will be entirely involved into G'. Thus our theorem has been proved. Similarly when $A(x)$ has the negative sign through the interval, the theorem will also hold.

In conclusion the author wishes to express his hearty thanks to Professor Toshizô Matsumoto for his kind remarks and to Mr. A. Kawaguchi for his kindness.

Graphical Computation of Jupiter's Perturbation on Asteroids[1)]

By

Joe Ueta

(Received November 29, 1934)

Abstract

For the computation of Jupiter's perturbation on Asteroids, a graphical method is recommended. It promises the computer easiness and sufficient accuracy for the derivation of data referred to the geometrical relation between Jupiter and Asteroids. The scale of the graph is a moderate one such that the orbit of Jupiter just fits on a sheet of typewriter paper.

Subsequent computation may be promptly carried out with a slide rule.

The coefficients of orbit improvement are also derived by a graphical method.

The incessant increase of the number of asteroids has compelled the "Astronomischen Rechen-Institut" at Berlin, Germany, to ask voluntary collaborations for the computation of Jupiter's perturbation on Asteroids. And Dr. Stracke of the Rechen-Institut has published instructions[2)] for the approximate calculation of special perturbation and for the improvement of orbital elements.

His method is that of the Variation of Elements which is generally treated in text books of theoretical astronomy, but Dr. Stracke has attained much simplification by using only three figure logarithms.

In view of the simplification, the computation also can be done with much easiness and moreover with sufficient accuracy by getting the necessary data for calculation with *graphical method* and by using a slide rule for the later computation. The scale of the graph may be a moderate one, such that the orbit of Jupiter can be graphed on a single sheet of typewriter paper.

1. An abstract of a part of this paper was read at the Annual Meeting of the Mathematico-Physical Society of Japan, Kyoto, 1931 October.

2. G. Stracke: Veröffentlichungen des Astronomischen Rechen-Instituts zu Berlin, Nr. 44.

The weak point of the graphical method generally lies in its inaccuracy, but here the required accuracy is within its limit. And without this defect, it is much superior to numerical calculation in a few points, especially where the geometrical transformation of coordinates is concerned. Of all merits of the graphical method, the fact that it is carried out in parallel, so that accidental mistakes are to be detected easily, should receive special mention.

In the following treatment the same notations are used as those given in Dr. Stracke's paper.

Elements:

M	Mean Anomaly	E	Eccentric Anomaly
M_0	Mean Anomaly at the instant t_0	v	True Anomaly
ω	Argument of Perihelion	r	Radius vector
Ω	Longitude of Ascending Node	p	Parameter of Orbit
i	Inclination of Orbit to the Ecliptic	u	Argument of Latitude
		L	Mean Longitude
φ	Angle of Eccentricity	π	Longitude of Perihelion
μ	Mean daily motion	k	Gauss's constant in degree
a	Semi-major axis	w	Time interval

λ_1 Heliocentric longitude of Jupiter
β_1 ,, latitude ,, ,,
r_1 Radius vector of Jupiter
m_1 Mass of Jupiter in unit of Sun's mass
S, T, W the components of the perturbing force

Then we have,

1) $$M=M_0+\mu(t-t_0)=L-\pi$$

2) $$E-\sin\varphi\sin E=M$$

3) $$\begin{cases} r\sin v=a\cos\varphi\sin E \\ r\cos v=a(\cos E-\sin\varphi) \end{cases}$$

4) $$a=\left(\frac{k}{\mu}\right)^{\frac{2}{3}}$$

5) $$u=v+\omega=v+\pi-\Omega$$

6) $$p=a\cos^2\varphi$$

7) $$\begin{cases} \cos B_1\cos L_1=\cos\beta_1\cos(\lambda_1-\Omega) \\ \cos B_1\sin L_1=\sin i\sin\beta_1+\cos i\cos\beta_1\sin(\lambda_1-\Omega) \\ \sin B_1\quad\ =\cos i\sin\beta_1-\sin i\cos\beta_1\sin(\lambda_1-\Omega) \end{cases}$$

$$8)\qquad \begin{cases} \xi_1 = r_1 \cos B_1 \cos(L_1 - u) \\ \eta_1 = r_1 \cos B_1 \sin(L_1 - u) \\ \zeta_1 = r_1 \sin B_1 \end{cases}$$

$$9)\qquad \rho_1^2 = r_1^2 + r^2 - 2r\xi_1$$

$$10)\qquad K = \frac{wkm_1}{\sqrt{p}}\left(\frac{1}{\rho_1^3} - \frac{1}{r_1^3}\right)$$

$$11)\qquad \begin{cases} S = K\xi_1 - \dfrac{wkm_1}{\sqrt{p}}\dfrac{r}{\rho_1^3} \\ T = K\eta_1 \\ W = K\zeta_1 \end{cases}$$

$$12)\qquad \begin{cases} w\dfrac{di}{dt} = r\cos u.\ W \\ w\dfrac{d\Omega}{dt} = \dfrac{r\sin u}{\sin i}.\ W \\ w^2\dfrac{d\mu}{dt} = -\dfrac{3kw}{\sqrt{a}}\sin\varphi\sin v.\ S - \dfrac{3kw}{\sqrt{a}}\dfrac{p}{r}.\ T \\ w\dfrac{d\pi}{dt} = -\dfrac{p}{\sin\varphi}\cos v.\ S + \dfrac{p+r}{\sin\varphi}\sin v.\ T + \tan\dfrac{i}{2}r\sin u.\ W \\ w\dfrac{dL}{dt} = -p\tan\dfrac{\varphi}{2}\cos v.\ S - 2\cos\varphi\ r.\ S \\ \qquad\qquad + \tan\dfrac{\varphi}{2}(p+r)\sin v.\ T + \tan\dfrac{i}{2}r\sin u.\ W \\ w\dfrac{d\varphi}{dt} = a\cos\varphi\sin v.\ S + a\cos\varphi\left[\sin\varphi + \cos v\left(1 + \dfrac{r}{a}\right)\right].\ T \end{cases}$$

Relative Positions of Jupiter and the Asteroid

We take the orbital plane of the asteroid as the fundamental plane of reference. Then the position of Jupiter can be represented by a point of orthogonal projection to the plane and the elevation above it.

For a while, considering the plane to be the ecliptic (in Fig. 1), let S be the position of the Sun, and a line $S\Upsilon$ be in the direction of the Vernal equinox. Draw a line SJ, making an angle λ_1 with the initial line $S\Upsilon$, and measure a curtate radius $r_1\cos\beta_1$ from S to J, then J is the projected position of Jupiter in the ecliptic, and it should be

understood that Jupiter lies just above that point as far as $r_1 \sin\beta_1$. If we describe a small circle h with a radius $r_1 \sin\beta_1$ about the point J, the elevation above the ecliptic (or the depression according to the case) may be clearly represented. For the sake of convenience of operation, $r_1 \cos\beta_1$ and $r_1 \sin\beta_1$ (in natural numbers) should be tabulated beforehand.

Fig. 1

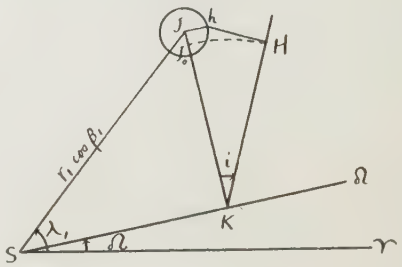

Next, draw the nodal line $S\Omega$ passing through the Sun, making an angle Ω with $S\Upsilon$, then we notice that the part of Jupiter's orbit, or strictly speaking, the part of the ecliptic which lies on the side of this line into which the asteroid passes the Ascending node, is below the fundamental plane. If we draw a normal JK from the point J to $S\Omega$, intersecting at K with it, we have

$$13) \qquad \begin{cases} JK = r_1 \cos\beta_1 \sin(\lambda_1 - \Omega) \\ SK = r_1 \cos\beta_1 \cos(\lambda_1 - \Omega). \end{cases}$$

Now let Jh be a radius of the small circle above mentioned, drawn parallel and in the same or opposite direction with $S\Omega$, according to whether Jupiter lies above or below the ecliptic, i. e. $r_1 \sin\beta_1$ is positive or negative.

Make a base line KH through the foot K and at an angle i with the line JK in the clockwise direction, and then draw a line perpendicularly to the base line KH from the point h. If we denote the intersection point with H, then we will see from the figure 1 that the distance KH is equal to $JK \cos i + Jh \sin i$, or

$$14) \qquad KH = r_1 \cos i \cos\beta_1 \sin(\lambda_1 - \Omega) + r_1 \sin i \sin\beta_1$$

and also that the perpendicular distance hH is equal to $JK \sin i - Jh \cos i$. And it will easily be seen that this distance is the depression of Jupiter under the fundamental plane, but since we measure the height of Jupiter above the fundamental plane positively, we must change the sign and we have

$$15) \qquad hH = r_1 \cos i \sin\beta_1 - r_1 \sin i \cos\beta_1 \sin(\lambda_1 - \Omega).$$

In the graphical method, the elevation or depression can be easily visualized by measuring the height from H to h positively towards S.

Now, if we describe a small arc with a radius KH and its centre

at K, cutting the line KJ at a point J_0, then the point J_0 represents the projected position of Jupiter on the fundamental plane. And join J_0 to S, then the angle ΩSJ_0 is nothing but the longitude in the fundamental plane. If we compare the equations (13), (14) and (15) with the equations (7), we will find easily that the angle has to be designated by L_1 and also that

$$SJ_0 = r_1 \cos B_1$$

$$hH = r_1 \sin B_1.$$

The position of the asteroid also can be drawn graphically. For that purpose, first compute the mean anomaly M for an epoch t by the formula (1) and then require the eccentric anomaly E, where it is sufficient to get E as accurate as one-tenth of a degree.

This process may be carried out very conveniently by the use of the Keplerian which gives the mechanical solution of Kepler's equation[1].

Now draw the apside line ASP (Fig. 2) through the Sun, making an angle ω with the nodal line $S\Omega$, and denote the Perihelion point and the Aphelion point by P and A which are distant from S by $a(1-\sin\varphi)$, $a(1+\sin\varphi)$ respectively.

Fig. 2

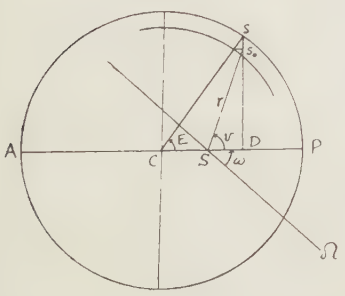

Then if we describe a circle with AP as its diameter, we can get the position of the asteroid in the following manner.

Take a point s on the periphery of the circle PsA, subtending an angle PCs at its centre C equal to E, and draw a normal to the apside line ASP passing the point s, and denote the foot of the normal by D. Now take a point of s_0 in the line sD dividing the normal in the ratio such that $sD : s_0D = 1 : \cos\varphi$, then s_0 is the true position of the asteroid in the orbit. Consequently, the distance Ss_0 is the radius vector r, and the angle PSs_0 is the true anomaly v.

$$\begin{cases} s_0D = r \sin v \\ SD = r \cos v \end{cases}$$

1. M. N. Vol. **87** p. 207.

and the angle measured from $S\Omega$ should be denoted by u.

Necessary data for the computation

In the figure 3, if we get a line J_0Q passing through the point J_0 perpendicular to the line Ss_0, then we have

$$16) \quad \begin{cases} SQ = SJ_0 \cos(L_1 - u) = r_1 \cos B_1 \cos(L_1 - u) \\ J_0Q = SJ_0 \sin(L_1 - u) = r_1 \cos B_1 \sin(L_1 - u). \end{cases}$$

And remembering the equations (8), we have the following relations:

$$\begin{cases} \xi_1 = SQ \\ \eta_1 = J_0Q \\ \zeta_1 = hH \end{cases}$$

where ξ_1 must be measured positively towards s_0; and η_1 is positive when J_0 proceeds s_0 in longitude i. e. J_0 lies in the left side of the direction Ss_0; about the sense of ζ_1, it has been already stated. To get the distance between Jupiter and the asteroid, first join the points J_0 and s_0, then the distance J_0s_0 expresses the projected distance in the fundamental plane. Now measure a distance J_0N equal to hH in (15) from J_0 perpendicularly to the line J_0s_0 and join the points N and s_0, then Ns_0 is the required distance ρ_1. Because it enters into the computation by the form of inverse cube, it is convenient to have a table of the inverse cube with the argument of ρ_1.

Fig. 3

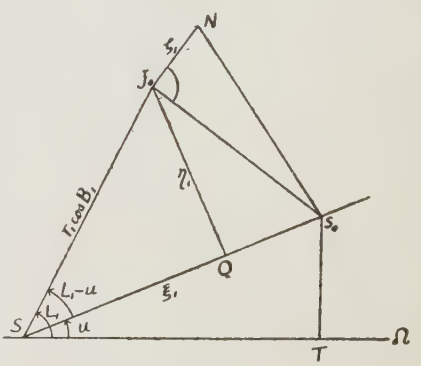

Other values necessary for the computation can be arrived at in the following manner:

Drawing a perpendicular s_0T from the point s_0 to the nodal line, measure the length of the perpendicular s_0T, and the distance from the Sun to the foot of the normal, ST; they give $r \sin u$ and $r \cos u$ respectively.

s_0T is positive when s_0 lies in the left side of the direction $S\Omega$, and ST must be measured positively along the direction of $S\Omega$.

Next, (Fig. 4) draw a circle around S with a unit radius, then it will cut the line Ss_0 or its elongation at U.

Fig. 4

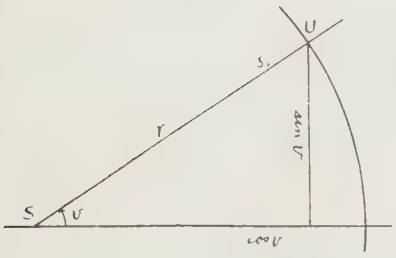

Then referring to the apside line, measure the normal and its offset in exactly the same way. They are nothing but $\sin v$ and $\cos v$ respectively.

Formulae of Perturbation

The formulae of perturbation (12) are rearranged for the convenience of the computation as follows; the modified form will be more profitable for the use of the slide rule, provided that the value of φ is not especially small.

$$K=\frac{wkm_1}{\sqrt{p}}\left(\frac{1}{\rho_1^3}-\frac{1}{r_1^3}\right) \qquad wkm_1=75.28 \text{ for } w=80$$

$$\begin{cases} S=K\xi_1-\dfrac{wkm_1}{\sqrt{p}}\dfrac{r}{\rho_1^3} \\ T=K\eta_1 \\ W=K\zeta_1 \end{cases}$$

$$\begin{cases} \delta i=r\cos u.\ W \\ \delta\Omega=\dfrac{r\sin u}{\sin i}.\ W \end{cases}$$

$$k_2=41.29$$

$$\begin{cases} 80\delta\mu_1=-\dfrac{k_2\sin\varphi}{\sqrt{a}}\sin v.\ S \\ 80\delta\mu_2=-\dfrac{k_2 p}{\sqrt{a}}\dfrac{1}{r}.\ T \end{cases}$$

$$\begin{cases} \delta\varphi_0=-\dfrac{1}{\tan\varphi}r.\ T \\ \delta\varphi_1=-\dfrac{a^{\frac{3}{2}}}{k_2\tan\varphi}.\ 80\delta\mu_1 \\ \delta\varphi_2=-\dfrac{a^{\frac{3}{2}}}{k_2\tan\varphi}.\ 80\delta\mu_2 \end{cases}$$

$$\begin{cases} \delta\pi_1=-\dfrac{p}{\sin\varphi}\cos v.\ S \\ \delta\pi_2=\dfrac{1}{\sin\varphi}(p+r)\sin v.\ T \\ \delta\pi_3=2\sin^2\dfrac{i}{2}.\ \delta\Omega \end{cases}$$

$$\begin{cases} \delta L_0=-2\cos\varphi\ r.\ S \\ \delta L_1=2\sin^2\dfrac{\varphi}{2}.\ \delta\pi_1 \\ \delta L_2=2\sin^2\dfrac{\varphi}{2}.\ \delta\pi_2 \\ \delta L_3=\delta\pi_3 \end{cases}$$

Example

Here is given an example of computation. The scale of the graph was such that the astronomical unit was represented in 2 centimeters, so the orbit of Jupiter fits on to a sheet of typewriter paper. The angles were measured with a celluloid protractor of ordinary size of 7 centimeters radius, consequently E and λ_1 were plotted within one tenth of a degree of accuracy.

For the purpose of comparison with Dr. Stracke's method, the same example as given in the "Veröffentlichungen" was taken:

(694) Ekard

$t_0 = 1909$ Dec. 3.5 U. T.

$M_0 = 46^\circ.350$

$\omega = 108.243$
$\Omega = 231.414$ } 1910.0
$i = 15.756$

$\varphi = 18.867$

$\mu = 813''.30 = 0^\circ.22592$

$\log a = 0.42650$

and the perturbation of Jupiter was calculated for the same interval, from the initial epoch up to 1922 Dec. 15.5 U. T.

The computation scheme follows in the pages 56–60, where we find it convenient to arrange the data in columns instead of in rows. Similarly to the example given by Dr. Stracke, the starting elements were not used all through the whole interval, from 1910 Jan. 12.5 to 1922 Dec. 15.5, but the elements were improved twice, namely first on 1915 Jan. 26.5 and next on 1920 Feb. 9.5. The corrections of the elements are calculated in the following way:

$$\Delta M = \Delta L_\mu + \Delta L - \Delta\pi$$

$$\Delta\omega = \Delta\pi - \Delta\Omega$$

$$M = M_0 + \mu^0(t - t_0) + \Delta M$$

$$\Delta a = -\frac{a}{120}\,\frac{80\Delta\mu^0}{\mu^0}$$

If we can use the summation table instead of the integration, then the value of ΔL_μ, corresponding to the first date of computation, will be

$$\Delta L_\mu(a) = {}^{II}F(a) + \frac{1}{12}F(a) - \frac{1}{240}F^{II}(a) + \cdots\cdots$$

and since $${}^{II}F(a) = \frac{1}{24}F(a-w) + \cdots\cdots$$

$$= \frac{1}{24}F(a) \text{ nearly,}$$

then $$\Delta L_\mu(a) = \frac{1}{8}F(a).$$

Comparison with the Observations

For the comparison with the observations, we can get the ephemerides with a graphical method. But in this case the graphical method is a little short, and a larger scale should be used to obtain more accuracy. It may not be out of place here to show the graphical method of getting the Right Ascension and Declination. Moreover, for the subsequent computation of the coefficients of the improvement of orbit, we can again take advantage of the graphical computation.

First, lay out a radius vector Ss_0 from the Sun S (Fig. 5) subtending an angle $u = v + \omega$ with the Nodal line $S\Omega$, and draw a normal s_0K to the line $S\Omega$ from the position of the asteroid s_0.

Fig. 5

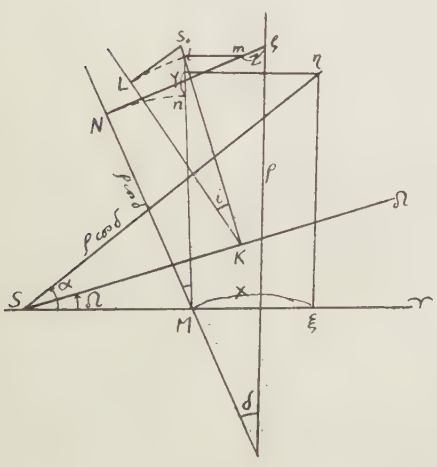

Then measure an angle i at K in the counter-clockwise direction and drop a normal from s_0 to the base line, let the foot be denoted by L. If we take a point l on the line Ks_0, such as

$$Kl = KL$$

then the point l is the projected position of the asteroid in the plane of the ecliptic. From l, draw a line lM perpendicularly to the equinoctial line $S\Upsilon$, and, in turn, another line lm perpendicularly to lM, and make $lm = Ls_0$.

lm is to be drawn in the direction of $S\Upsilon$, when s_0 is in the side of Ω referred to LK, and if otherwise to the opposite.

Next, pass a line MN through M, making an angle ε in the counter-clockwise direction with Ml, then if we draw a normal from the point m to the line intersecting at N with it, we have

$$\begin{cases} x=SM \\ y=MN \\ z=Nm. \end{cases}$$

SM is measured as positive when M lies in the direction $S\Upsilon$, MN is positive when N lies in the lefthand side of the direction from S to Υ. Nm is positive when m is in the same side with Υ referred to MN.

When we add X, Y, and Z to these values of x, y and z respectively, we get $\rho\cos\delta\cos\alpha$, $\rho\cos\delta\sin\alpha$, $\rho\sin\delta$, and the subsequent process to get α, δ and ρ is easily seen from the figure.

Computation of the factors of "Bahnverbesserung".

When we are given with $t-t_0$, M, E and the orbital elements, we get graphically r, $\sin v$, so we can compute the coefficients l, m, n, and o with a slide rule by the following formulae:

$$\begin{cases} l=\dfrac{a\cos\varphi\dfrac{a}{r}(t-t_0)}{3600}\cdot\dfrac{1}{\rho}=\dfrac{t-t_0}{3600}o \\ m=\dfrac{(p+r)\sin v}{\cos\varphi}\cdot\dfrac{1}{\rho} \\ n=\dfrac{r}{\rho} \\ o=a\cos\varphi\dfrac{a}{r}\cdot\dfrac{1}{\rho} \end{cases}$$

$\sin F$ and $\cos F$ which are necessary for the computation of the absolute term can be derived graphically by the following process:

In Fig. 6, taking a point g on $S\Omega'$, distant from the Sun by $\rho\sin\delta$, close a rectangle with $g\eta$ as its diagonal and with a part of $S\eta$ as one side. Denote the angular point by h. Here we must be careful to measure the length Sg in the opposite direction when $\rho\sin\delta$ is negative. Next, pass a base line through S, making an angle i' with $S\eta$ in the clockwise direction, and project the point h to the base line, then the offset SH of the normal gives

$$\rho\cos i'\cos\delta+\rho\sin i'\sin\delta\sin(\alpha-\Omega')$$

which is expressed by $\rho\cos g\cos F$.

Again, taking a point k on $S\Omega'$, distant from the Sun by ρ, drop a normal kK to the line $S\eta$ through k. Subsequently, make a line parallel to SH through the point K and let it intersect with the line hH or its elongation. If we denote the intersection point with F, then the angle HSF is the required angle F. F is measured positively in the counter-clockwise direction from SH.

Fig. 6

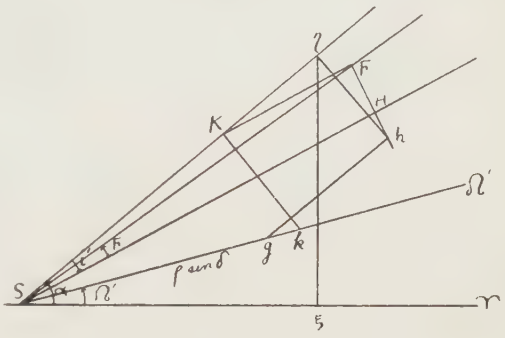

The process may be carried out as the continuation of the preceding article. In that occasion, we must be careful to distinguish Ω', i' from Ω, i, the former set of which are the Right Ascension of the Ascending Node and Inclination of the orbit referred to the equator and the latter are those referred to the ecliptic.

To correct the position of the nodal line, the best way is first to find i', the inclination of the orbit to the equator.

Fig. 7

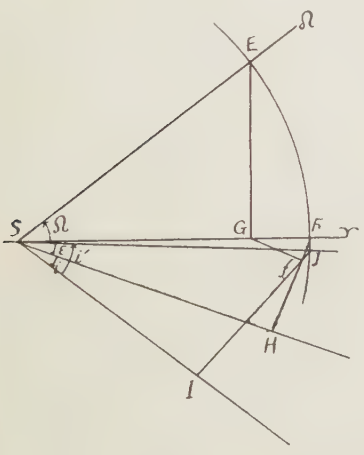

Describe an arc of circle of a unit radius, having its centre at S, and cut the nodal line $S\Omega$ and the Vernal line $S\Upsilon$ at E and F respectively. Next draw a normal through E to the Vernal line $S\Upsilon$, and let it be intersected with it at G.

Then subtend two lines SH, SI, making angles ε, $\varepsilon+i$ respectively with $S\Upsilon$ at S. Now drop a normal through F to the line SH intersecting at H, and drawing a line through G and parallel to SH, cut FH at f.

And subsequently, a normal to the line SI through f is to be drawn.

Then SI gives $\cos i'$, so if we cut the line If or its elongation at J with a unit radius from S, then the angle JSI is equal to i'.

Referring to the same diagram, but to Fig. 8, draw a line GK

through the point G making an angle ε with GE. Drop a normal from the point E to GK, intersecting at K. If we draw a line EN through E, making an angle $90-i'$ with the normal EK to the side of G, then it will cut the base line GK or its elongation at N. Then NK gives the equatorial distance (say) between the nodes of the equator and of the ecliptic. The alternative to get the length NK is to obtain the base line corresponding to a side, equal to EK, which subtends the angle JSI in Fig. 7.

The next step is thus: cut the normal GE at L with a radius equal to GK, and its centre at G. Then describe a circle, having SL as its diameter, and cut off a chord LM equal to KN, in the side nearer to Υ, then the line joining M and S gives the position of the nodal line in the equator. It should be noted here that in such a case where the normal from E to the equinoctial line does not meet with it in the branch of $S\Upsilon$, i. e. it falls on the Autumnal line $S\Upsilon'$, then substitute the diametrical line of the nodal line, and proceed in the same way as above, except that SI (in Fig. 7) is to be laid so as to make an angle $\varepsilon-i$, instead of $\varepsilon+i$.

Following remarks should be given here, to cover special cases.

a) Although it is not generally the case for asteroids to have a large value of i, there are sometimes cases where i is so large that the normal from the point f (Fig. 7) does not meet with the line SI, then substitute the diametrical line of SI.

b) And when the normal from the point f to the line SI or its substitute, is averted from SH line, then we should measure the chord LM in the semi-circle of the further side with respect to Υ.

c) With regard to the sense of the required nodal line, it should be noted that when Ω lies in the first two quadrants, then Ω' is to be taken either in the first or in the second quadrant, and when Ω lies in the last two quadrants, then Ω' is in the third or in the fourth quadrant.

d) When NK is equal to LS in length, the chord LM coincides with the diameter of the circle, and the position of the nodal line seems to be indeterminate, but it means that the nodal line is to be laid perpendicularly to the line LS. And when it is nearly the case, a small error in the length NK will affect the direction of Ω' very much, so it is recommended to use another method for an alternative. The process is thus: In Fig. 7 and 9, close a rectangle with F, f and G, and denote the new angular point by g, and let the line SH be

elongated to intersect with the unit circle at h, then draw two normals gP, hQ to SI through the points g, h respectively.

If we cut fragments Sp in $S\Upsilon$, and Sq in $S\Omega$, respectively equal to gP and hQ, then the point o which is given by the intersection of the normal and the parallel to SF through p and q, will give the direction Ω', by joining S, o. Sq should be measured always towards Ω, but Sp is measured towards Υ for the value of i, as far as the line SI or its diametrical line passes the point g, starting from the line SH, and for the larger value of i, Sp is measured to the opposite.

Fig. 8

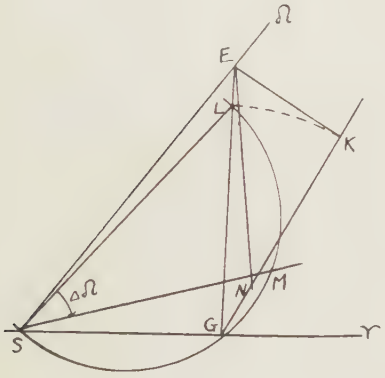

Fig. 9

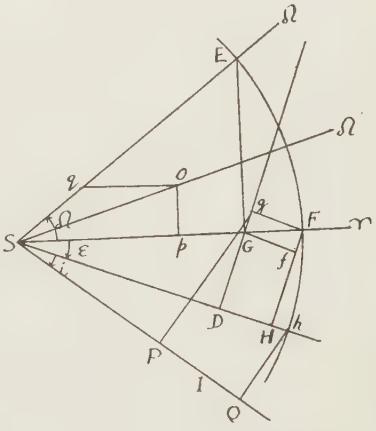

The above process will be approved by geometrical consideration, but may be verified in the following way.

Referring to the figure 10, we have the trigonometrical relations between these spacial elements as follows:

$$17)\quad \begin{cases} \sin i' \sin\Omega' = \sin i \sin\Omega \\ \sin i' \cos\Omega' = \cos i \sin\varepsilon + \sin i \cos\varepsilon \cos\Omega \\ \cos i' = \cos i \cos\varepsilon - \sin i \sin\varepsilon \cos\Omega \\ \sin\Delta\Omega = \tan b \cot i' \\ \sin b = \sin\Omega \sin\varepsilon \end{cases}$$

Fig. 10

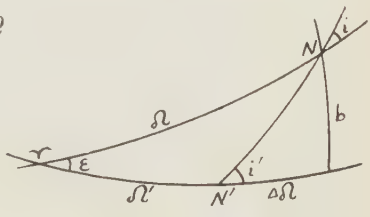

When we refer to Figure 7

$$\Upsilon S\Omega = \Omega$$

and as SE, SF were taken as unit length,

$$SG=\cos\Omega$$
$$fH=SG\sin\varepsilon=\cos\Omega\sin\varepsilon$$
$$SH=SF\cos\varepsilon= \quad \cos\varepsilon$$
$$SI=SH\cos i-fH\sin i$$
$$=\cos i\cos\varepsilon-\sin i\sin\varepsilon\cos\Omega,$$

so, $SI=\cos i'$, and since $SJ=1$

$$\angle JSI=i'.$$

And now we have, in Fig. 8

$$EG=\sin\Omega$$
$$EK=EG\sin\varepsilon=\sin\Omega\sin\varepsilon$$
$$KN=EK\cot i'=\frac{\sin\Omega\sin\varepsilon}{\tan i'}=LM$$
$$GK=GL=EG\cos\varepsilon=\sin\Omega\cos\varepsilon$$
$$SG=\cos\Omega$$

Consequently, $SL^2=SG^2+GL^2=\cos^2\Omega+\sin^2\Omega\cos^2\varepsilon$
and

$$1-SL^2=1-\cos^2\Omega-\sin^2\Omega\cos^2\varepsilon=\sin^2\Omega\sin^2\varepsilon,$$

that is equal to $\sin^2 b$ from the trigonometrical relation (17).
Thence, we have $SL=\cos b$.

In the rectangular triangle LSM,

$$\sin LSM=\frac{LM}{SL}=\frac{\sin\Omega\sin\varepsilon}{\tan i'}\cdot\frac{1}{\cos b}=\frac{\tan b}{\tan i'}$$

or equal to $\sin\Delta\Omega$ from the same trigonometrical relation (17).

Consequently, we have

$$\angle LSM=\Delta\Omega$$

and SL is the projection of the nodal line $S\Omega$ in the ecliptic to the plane of the equator, so we can see ΥSM corresponds to Ω'.

In Fig. 9,

$$gD=FH=SF\sin\varepsilon=\sin\varepsilon$$
$$SD=SG\cos\varepsilon=\cos\Omega\cos\varepsilon$$
$$gP=gD\cos i+SD\sin i=\cos i\sin\varepsilon+\sin i\cos\varepsilon\cos\Omega,$$

so, $gP=\sin i'\cos\Omega'$ from the equation (17).

$$Sq=hQ=Sh\sin i=\sin i$$
$$op=Sq\sin\Omega=\sin i\sin\Omega=\sin i'\sin\Omega'$$

consequently, we have

$$\angle oSp=\Omega'.$$

Example for the Computation of the Coefficients

Thorough comparison of the computation for all the dates with that given by Dr. Stracke seems to be unnecessary. Here we show the comparison of both the methods for a single date,

1913 Aug. 2.0

for which,

$t-t_0$	$1337^d.5$	
M	$348^\circ.78$	
ω	108.00	1913.0
Ω	231.44	1913.0
i	15.75	1913.0
φ	18.83	
a	2.67	
ε	$23^\circ.45$	

are given.

We compute $b=2.53$ $p=2.39$ $ae=0.86$ $E=-16^\circ.4$

and by the graphical construction, we read out the necessary data for computation as follows:

		Dr. Stracke's computation
r	1.84	1.845
$\sin v$	− .389	− .387
x	+1.284	+1.2857
y	−1.316	−1.3213
z	− .032	− .0294
α	$317^\circ.3$	$317^\circ.18$
δ	+18.0	+17.88
ρ	.920	.925

and the subsequent computation with a slide rule gives,

l	+1.48	+1.47
m	−1.89	−1.87
n	+2.00	+2.00
o	+3.99	+3.96

With regard to F, Dr. Stracke accidentally mistook Ω, i as the elements referred to the ecliptic instead of as those referred to the equator.

But for the purpose of comparison, the same values of Ω, i were used, resulting the following values

		Dr. Stracke's
$\sin F$	+ .020	+ .021
$\cos F$	+1.00	+1.000

Kyoto University Observatory, October, 1934

Tables

Data for the construction of the graph

Orbital constants		0.5 U. T.		M	E
				°	°
	1	1910 **1** 12		55.39	73.1
	2	**4** 2		73.46	92.0
	3	**6** 21		91.53	109.0
	4	**9** 9		109.61	124.8
a 2.670	5	**11** 28		127.68	139.7
$\sin\varphi$ .3234	6	1911 **2** 16		145.75	153.9
	7	**5** 7		163.82	167.8
$\cos\varphi$ .9463	8	**7** 26		181.90	−178.6
	9	**10** 14		199.97	−164.9
ae .863					
	10	1912 **1** 2		218.04	−151.0
b 2.53	11	**3** 22		236.12	−136.6
	12	**6** 10		254.19	−121.6
p 2.39	13	**8** 29		272.26	−105.6
	14	**11** 17		290.34	−88.2
	15	1913 **2** 5		308.41	−68.9
	16	**4** 26		326.48	−47.1
	17	**7** 15		344.56	−22.6
	18	**10** 3		2.63	3.9
	19	**12** 22		20.70	30.0
	20	1914 **3** 12		38.77	53.7
	21	**5** 31		56.85	74.7
	22	**8** 19		74.92	93.4
	23	**11** 17		92.99	110.4
	24	1915 **1** 26		111.07	126.0

Factors for the subsequent computation

$\frac{k_1}{\sqrt{p}}$	48.70	$\frac{k_2\sin\varphi}{\sqrt{a}}$	$\frac{1}{.1224}$
$\tan\varphi$	.3417	$\frac{k_2 p}{\sqrt{a}}$	60.40
$2\cos\varphi$	$\frac{1}{.5284}$	$\frac{a^{\frac{3}{2}}}{k_2\tan\varphi}$	.3092
$2\sin^2\frac{\varphi}{2}$	.0537	$\sin i$	.2715
$\frac{p}{\sin\varphi}$	$\frac{1}{.1353}$	$2\sin^2\frac{i}{2}$	.0375

	0.5 U.T.			ρ_1	ξ_1	η_1	ζ_1	r	$r\sin u$	$r\cos u$	$\sin v$	$\cos v$
1	1910	1	12	6.76	−2.11	4.87	1.20	2.42	−.84	−2.28	1.000	−.039
2		4	2	6.52	−1.01	5.25	1.10	2.70	−1.69	−2.10	.937	−.351
3		6	21	6.30	−.18	5.38	.97	2.95	−2.39	−1.73	.811	−.583
4		9	9	6.05	.50	5.36	.83	3.16	−2.91	−1.22	.659	−.752
5		11	28	5.84	.99	5.30	.69	3.34	−3.26	−.65	.499	−.870
6	1911	2	16	5.60	1.45	5.21	.54	3.45	−3.45	−.05	.330	−.947
7		5	7	5.37	1.84	5.10	.40	3.51	−3.46	+.58	+.158	−.989
8		7	26	5.13	2.20	4.95	.22	3.54	−3.33	1.18	−.018	−1.000
9		10	14	4.87	2.53	4.77	.06	3.51	−3.05	1.73	−.190	−.983
10	1912	1	2	4.59	2.86	4.56	−.10	3.44	−2.65	2.18	−.360	−.936
11		3	22	4.29	3.20	4.28	−.27	3.31	−2.12	2.54	−.529	−.852
12		6	10	3.96	3.60	3.91	−.43	3.14	−1.48	2.77	−.692	−.727
13		8	29	3.61	4.03	3.40	−.60	2.92	−.73	2.82	−.841	−.547
14		11	17	3.32	4.50	2.68	−.74	2.66	+.05	2.67	−.955	−.300
15	1913	2	5	3.12	4.95	1.54	−.88	2.36	.83	2.23	−1.000	+.044
16		4	26	3.21	5.13	−.10	−1.02	2.08	1.50	1.47	−.890	.460
17		7	15	3.65	4.59	−2.18	−1.14	1.87	1.83	+.44	−.526	.855
18		10	3	4.45	2.79	−4.16	−1.24	1.80	1.65	−.73	+.102	.996
19		12	22	5.31	.47	−4.94	−1.32	1.93	.98	−1.65	.660	.752
20	1914	3	12	6.07	−1.40	−4.72	−1.38	2.16	+.05	−2.16	.943	+.339
21		5	31	6.66	−2.63	−4.10	−1.40	2.45	−.92	−2.28	1.000	−.066
22		8	19	7.12	−3.31	−3.50	−1.42	2.73	−1.76	−2.08	.928	−.375
23		11	17	7.50	−3.75	−3.00	−1.42	2.97	−2.45	−1.68	.797	−.603
24	1915	1	26	7.79	−4.03	−2.58	−1.41	3.18	−2.95	−1.16	+.643	−.764

	$\frac{1}{\rho_1^3}$	$\frac{1}{r_1^3}$	$\frac{1}{\rho_1^3}-\frac{1}{r_1^3}$	K	$K\xi_1$	$T=K\eta_1$	$W=K\zeta_1$	$\frac{1}{.2053}\frac{k_1}{\sqrt{p}}\frac{r}{\rho_1^3}$	S
1	.00324	.00617	−.00293	−.1427	+.301	−.695	−.1712	.382	−.081
2	361	617	256	−.1246	.1258	−.654	−.1370	.476	−.350
3	400	617	217	−.1056	+.0190	−.568	−.1025	.575	−.556
4	452	618	166	−.0809	−.0405	−.434	−.0672	.696	−.7365
5	502	620	118	−.0575	−.0569	−.305	−.0397	.818	−.875
6	.00569	623	−.00054	−.0263	−.0372	−.137	−.0142	.9575	−.995
7	646	627	+.00019	+.0093	+.0171	+.0474	+.00372	1.106	−1.089
8	741	632	109	.0531	.1167	.2624	.01166	1.276	−1.159
9	866	638	228	.1110	.2809	.530	+.00667	1.479	−1.198
10	.01034	645	389	.1894	.542	.864	−.01894	1.735	−1.193
11	1266	653	613	.2984	.956	1.278	−.0807	2.044	−1.088
12	1610	662	948	.462	1.66	1.804	−.1984	2.466	−.806
13	2126	672	1454	.708	2.85	2.406	−.425	3.027	−.174
14	2733	682	2051	.998	4.49	2.673	−.738	3.543	+.947
15	.03293	693	2600	1.266	6.27	+1.950	−1.113	3.787	2.483
16	3023	705	2318	1.128	5.80	−.1128	−1.151	3.067	2.732
17	2056	716	1340	.653	3.00	−1.423	−.745	1.870	+1.130
18	1135	729	+.00406	+.1975	+.551	−.8215	−.245	.995	−.444
19	668	741	−.00073	−.0355	−.0170	+.1753	+.0468	.628	−.645
20	.00447	753	306	−.149	+.2088	.7038	.2056	.471	−.262
21	338	765	427	−.208	.5473	.8532	.2912	.404	+.143
22	277	776	499	−.2432	.805	.8518	.3454	.369	.436
23	237	787	550	−.268	1.005	.805	.3808	.343	.662
24	.00212	.00796	−.00584	−.2844	+1.147	+.735	+.4015	.328	+.819

			$\frac{1}{.1224}$	-60.40		$-.3417$	$-.3092$	
	δi	$\delta\Omega$	$80\delta\mu_1$	$80\delta\mu_2$	$80\delta\mu$	$\delta\varphi_0$	$\delta(\varphi_1+\varphi_2)$	δp
1	+.39	+.53	+.65	+17.35	+18.00	+4.92	−5.56	−.64
2	.29	.85	2.68	14.63	17.31	5.17	−5.35	−.18
3	.18	.90	3.68	11.63	15.31	4.91	−4.74	+.17
4	.08	.72	3.96	8.30	12.26	4.02	−3.79	.22
5	.03	.48	3.57	5.52	9.09	2.98	−2.81	+.17
6	.00	+.18	2.68	+2.40	5.08	+1.38	−1.57	−.19
7	.00	−.05	+1.41	−.82	+.59	−.49	−.18	−.67
8	.01	−.14	−.17	−4.48	−4.65	−2.72	+1.44	−1.28
9	+.01	−.08	−1.86	−9.12	−10.98	−5.44	3.40	−2.04
10	−.04	+.19	−3.51	−15.16	−18.67	−8.70	5.77	−2.93
11	−.25	.63	−4.70	−23.33	−28.03	−12.38	8.67	−3.71
12	−.55	1.08	−4.56	−34.7	−39.26	−16.58	12.13	−4.45
13	−1.34	+1.14	−1.19	−49.8	−50.99	−20.60	15.74	−4.86
14	−1.97	−.14	+7.49	−60.7	−53.21	−20.80	16.45	−4.35
15	−2.48	−3.40	20.28	−49.9	−29.62	−13.47	+9.16	−4.31
16	−1.69	−6.37	19.84	+3.28	+23.12	+.69	−7.15	−6.46
17	−.33	−5.02	4.86	46.0	50.86	7.80	−15.71	−7.91
18	−.18	−1.49	.37	+27.56	+27.93	+4.33	−8.64	−4.31
19	−.08	+.17	3.47	−5.48	−2.01	−.99	+.62	−.37
20	−.44	+.04	+2.02	−19.80	−17.78	−4.45	5.50	+1.05
21	−.66	−.99	−1.17	−21.02	−22.19	−6.12	6.86	.74
22	−.72	−2.24	−3.30	−18.84	−22.14	−6.80	6.85	+.05
23	−.64	−3.44	−4.32	−16.36	−20.68	−7.00	6.40	−.60
24	−.46	−4.36	−4.31	−13.95	−18.26	−6.84	+5.65	−1.20

	$\frac{1}{.1353}$			.3234		.0375		$\frac{1}{.5284}$	.0537	
	$\delta\pi_1$	$p+r$	$(p+r)\sin v$	$\delta\pi_2$	$\delta(\pi_1+\pi_2)$	$\delta\pi_3=\delta L_3$	$\delta\pi$	δL_0	$\delta(L_1+L_2)$	δL
1	−.02	4.81	+4.81	−10.35	−10.37	+.02	−10.35	+.37	−.56	−.17
2	−.91	5.09	4.77	−9.65	−10.56	3	−10.53	1.79	−.57	+1.25
3	−2.40	5.34	4.33	−7.61	−10.01	3	−9.98	3.11	−.54	2.60
4	−4.09	5.55	3.66	−4.91	−9.00	3	−8.97	4.41	−.48	3.96
5	−5.62	5.73	2.86	−2.70	−8.32	2	−8.31	5.53	−.45	5.10
6	−6.96	5.84	1.93	−.82	−7.78	+.01	−7.76	6.50	−.42	6.09
7	−7.96	5.90	+.933	+.14	−7.82	0	−7.82	7.24	−.42	6.82
8	−8.56	5.93	−.107	−.09	−8.65	−.01	−8.66	7.76	−.46	7.29
9	−8.71	5.90	−1.12	−1.84	−10.55	0	−10.55	7.96	−.57	7.39
10	−8.26	5.83	−2.10	−5.60	−13.86	+.01	−13.85	7.78	−.74	7.05
11	−6.85	5.70	−3.02	−11.92	−18.77	2	−18.75	6.82	−1.01	5.83
12	−4.33	5.53	−3.83	−21.38	−25.71	4	−25.67	4.80	−1.38	+3.46
13	−.70	5.31	−4.46	−33.20	−33.90	+.04	−33.86	+.96	−1.82	−.82
14	+2.10	5.05	−4.82	−39.80	−37.70	0	−37.70	−4.77	−2.02	−6.79
15	−.81	4.75	−4.75	−28.60	−29.41	−.13	−29.54	−11.10	−1.58	−12.81
16	−9.28	4.47	−3.98	+1.39	−7.89	−.24	−8.13	−10.76	−.42	−11.42
17	−7.15	4.26	−2.24	+9.86	+2.71	−.19	+2.52	−4.01	+.15	−4.05
18	+3.27	4.19	+.43	−1.09	2.18	−.06	2.12	+1.51	.12	+1.57
19	3.58	4.32	2.85	+1.35	5.13	+.01	5.14	2.36	.28	2.65
20	.66	4.55	4.29	9.35	10.01	0	10.01	+1.07	.54	+1.61
21	.07	4.84	4.84	12.76	12.83	−.04	12.79	−.66	.69	−.01
22	1.21	5.12	4.75	12.50	13.71	−.08	13.63	−2.25	.74	−1.59
23	2.95	5.36	4.27	10.63	13.60	−.13	13.47	−3.73	.73	−3.13
24	+4.62	5.57	+3.58	8.14	+12.76	−.16	+12.60	−4.93	+.69	−4.40

12h U.T.	$80\delta_\mu$	$80\Delta_\mu$	ΔZ_μ	δZ	ΔZ	$\delta\pi$	$\Delta\pi$	$\delta\rho$	$\Delta\rho$	$\delta\Omega$	$\Delta\Omega$	δi	Δi	12h U.T.
														1909
		°			°.000		°.000		°.000		°.000		°.000	12 3
1910														1910
1 12	18		°			−10		−1		1		0		
4 2	17	18	*.0009	0	.000	−11	−.010	0	−.001	1	.001	0	.000	2 21
6 21	15	35	.0027	1	.001	−10	−.021	0	−.001	1	.002	0	.000	5 12
9 9	12	50	.0062	3	.004	−9	−.031	0	−.001	1	.003	0	.000	7 31
11 28	9	62	.0112	4	.008	−8	−.040	0	−.001	0	.004	0	.000	10 19
			.0174	5										
1911														1911
2 16	5	71		6	.013	−8	−.048	0	−.001	0	.004	0	.000	1 7
5 [illegible]	1	76	.0245	7	.019	−8	−.056	−1	−.001	0	.004	0	.000	3 28
7 26	−5	77	.0321	7	.026	−9	−.064	−1	−.002	0	.004	0	.000	6 16
10 14	−11	72	.0398	7	.033	−11	−.073	−2	−.003	0	.004	0	.000	9 4
		61	.0470	7	.040		−.084		−.005		.004		.000	11 23
1912														1912
1 2	−19					−14		−3		0		0		
3 22	−28	42	.0531	7	.047	−19	−.098	−4	−.008	1	.004	0	.000	2 11
6 10	−39	14	.0573	6	.053	−26	−.117	−4	−.012	1	.005	−1	.000	5 1
8 29	−51	−25	.0587	3	.056	−34	−.143	−5	−.016	1	.006	−1	−.001	7 20
11 17	−53	−76	.0562	−1	.055	−38	−.177	−4	−.021	0	.007	−2	−.002	10 8
		−129	.0486	−7	.048		−.215		−.025		.007		−.004	12 27
1913														1913
2 5	−30					−30		−4		−3		−2		
4 26	23	−159	.0357	−13	.035	−8	−.245	−6	−.029	−6	.004	−2	−.006	3 17
7 15	51	−136	.0198	−11	.024		−.253	−8	−.035	−5	−.002	0	−.008	6 5
10 3	28	−85	.0062	−4	.020	3	−.250	−4	−.043	−5	−.007	0	−.008	8 24
12 22	−2	−57	−.0023	2	.022	2	−.248	0	−.047	−1	−.008	0	−.008	11 12
			−.0080	3		5				0		0	−.008	
1914														1914
3 12	−18	−59		2	.025	10	−.243	1	−.047	0	−.008	0	−.008	1 31
5 31	−22	−77	−.0139	0	.027	13	−.233	1	−.046	0	−.008	−1	−.008	4 21
8 19	−22	−99	−.0216	−2	.027	14	−.220	0	−.045	−1	−.009	−1	−.009	7 10
11 7	−21	−121	−.0315	−3	.025	13	−.206	−1	−.045	−2	−.011	−1	−.010	9 28
		−142	−.0436		.022		−.193		−.046	−3	−.014		−.011	12 17
1915														1915
1 26	−19					13	−.180	−1	−.047	−4	−0.18	0	−.011	3 7
4 16	−16	−161	−.0578	−4	.018	12	−.168	−2	−.049	−5	−.023	0	−.011	5 26
7 5	−14	−177	−.0739	−5	.013	10	−.158	−2	−.051	−5	−.028	0	−.011	8 14
9 23	−12	−191	−.0916	−6	.007	9	−.149	−3	−.054	−5	−.033	0	−.011	11 2
12 12	−9	−203	−.1107	−7	.000	8		−3		−4		0		
			−.1310	−7										
1916														1916
3 1	−7	−212												
		−219	−.1522	−7	−.007	6	−.141	−3	−.057	−4	−.037	1	−.011	1 21
5 20	−4	−223	−.1741	−7	−.014	5	−.135	−3	−.060	−3	−.041	1	−.010	4 10
8 8	−1	−224	−.1964	−7	−.021	5	−.130	−3	−.063	−3	−.044	1	−.009	6 29
10 27	3	−221	−.2188	−7	−.028	4	−.126	−3	−.066	−2	−.046	1	−.008	9 17
					−.035	4	−.122	−3	−.069	−1	−.047	0	−.008	12 6

* Refer to the page 49.

12h U.T.	80δμ	80Δμ	ΔLμ	δL	ΔL	δπ	Δπ	δρ	Δρ	δΩ	ΔΩ	δi	Δi	12h U.T.
1917														1917
			°		°		°		°		°		°	
1 15	8		−.2409	− 6	−.041	4	−.118	− 3	−.072	0	−.047	0	−.008	2 24
4 5	13	−213	−.2622	− 5	−.046	5	−.113	− 3	−.075	0	−.047	0	−.008	5 15
6 24	19	−200	−.2822	− 4	−.050	6	−.107	− 3	−.078	0	−.047	0	−.008	8 3
9 12	25	−181	−.3003	− 2	−.052	7	−.100	− 3	−.081	0	−.047	0	−.008	10 22
12 1	24	−156	−.3159	0		5		− 3		0		0		
1918														1918
		−132			−.052		−.095		−.084		−.047		−.008	1 10
2 19	7	−125	−.3291	2	−.050	4	−.091	− 1	−.085	0	−.047	0	−.008	3 31
5 10	−26	−151	−.3416	3	−.047	12	−.079	3	−.082	0	−.047	0	−.008	6 19
7 29	−59	−210	−.3567	− 1	−.048	25	−.054	6	−.076	0	−.047	− 1	−.009	9 7
10 17	−79	−289	−.3777	−10	−.058	37	−.017	7	−.069	− 5	−.052	− 3	−.012	11 26
1919														1919
1 5	−68		−.4066	−22	−.080	35	.018	9	−.060	−17	−.069	− 5	−.017	2 14
3 26	−29	−357	−.4423	−32	−.112	20	.038	12	−.048	−35	−.104	− 6	−.023	5 5
6 14	15	−386	−.4809	−34	−.146	5	.043	16	−.032	−49	−.153	− 5	−.028	7 24
9 2	46	−371	−.5180	−30	−.176	− 2	.041	20	−.012	−56	−.209	− 3	−.031	10 12
11 21	64	−325	−.5505	−23	−.199	− 1	.040	22	.010	−55	−.264	0	−.031	12 31
		−261												
1920														1920
2 9	70		−.5766	−15	−.214	4	.044	21	.031	−47	−.311	3	−.028	3 20
4 29	69	−191	−.5957	−10	−.224	12	.056	20	.051	−39	−.350	4	−.024	6 8
7 18	64	−122	−.6079	− 5	−.229	19	.075	17	.068	−29	−.379	5	−.019	8 27
10 6	56	− 58	−.6137	− 1	−.230	23	.098	14	.082	−18	−.397	4	−.015	11 15
12 25	49	− 2	−.6139	1		26		11		−11		4		
1921														1921
		47			−.229		.124		.093		−.408		−.011	2 3
3 15	39	85	−.6092	3	−.226	23	.147	7	.100	− 5	−.413	3	−.008	4 24
6 3	26	112	−.6007	4	−.222	18	.165	4	.104	− 1	−.414	2	−.006	7 13
8 22	15	127	−.5895	4	−.218	12	.177	2	.106	0	−.414	1	−.005	10 1
11 10	1	128	−.5768	3	−.215	4	.181	2	.108	0	−.414	0	−.005	12 20
1922														1922
1 29	−12	116	−.5640	2	−.213	− 1	.180	2	.110	0	−.414	0	−.005	3 10
4 19	−19	97	−.5524	0	−.213	− 3	.177	3	.113	− 1	−.415	0	−.005	5 29
7 8	−16	81	−.5427	− 2	−.215	− 2	.175	3	.116	− 1	−.416	0	−.005	8 17
9 26	− 6		−.5346	− 3	−.218	− 3	.172	2	.118	0	−.416	0	−.005	11 5
12 15	3	75	−.5271	− 3		− 6		1		0		0		

Jupiter's Co-ordinates.

Date 12h U.T.			λ_1	$r_1[\cos\beta_1]$	$r_1\sin\beta_1$	$\frac{10^5}{r_1^3}$	Date 12h U.T.			λ_1	$r_1[\cos\beta_1]$	$r_1\sin\beta_1$	$\frac{10^5}{r_1^3}$
			°							°			
1910	1	12	183.8	5.45	+.12	617	1920	2	9	133.6	5.32	+.07	664
	4	2	189.8	5.45	.12	617		4	29	140.0	5.34	.08	655
	6	21	195.9	5.45	.12	617		7	18	146.2	5.37	.09	644
	9	9	201.9	5.45	.12	618		10	6	152.4	5.39	.10	640
	11	28	208.0	5.44	.12	620		12	25	158.6	5.40	.11	634
1911	2	16	214.1	5.43	+.11	623	1921	3	15	164.8	5.42	+.11	628
	5	7	220.2	5.42	.11	627		6	3	170.9	5.43	.12	624
	7	26	226.3	5.41	.10	632		8	22	177.0	5.44	.12	620
	10	14	232.5	5.39	.09	638		11	10	183.0	5.45	.12	618
1912	1	2	238.7	5.37	+.08	645	1922	1	29	189.1	5.45	+.12	617
	3	22	244.9	5.35	.07	653		4	19	195.1	5.45	.12	616
	6	10	251.2	5.33	.06	662		7	8	201.2	5.45	.12	617
	8	29	257.6	5.30	.04	672		9	26	207.2	5.45	.12	619
	11	17	264.0	5.27	.03	682		12	15	213.3	5.44	.11	622
1913	2	5	270.5	5.24	+.02	693	1923	3	5	219.4	5.43	+.11	625
	4	26	277.1	5.22	0	705		5	24	225.5	5.41	.10	630
	7	15	283.8	5.19	−.01	717		8	12	231.7	5.40	.09	636
	10	3	290.5	5.16	−.02	729		10	31	237.9	5.38	.08	643
	12	22	297.3	5.13	−.04	741	1924	1	19	244.1	5.36	+.07	650
1914	3	12	304.2	5.10	−.05	753		4	8	250.4	5.33	.06	659
	5	31	311.1	5.08	.06	765		6	27	256.7	5.31	.05	668
	8	19	318.1	5.05	.07	776		9	15	263.1	5.28	.04	678
	11	7	325.2	5.03	.08	787		12	4	269.6	5.26	.02	689
1915	1	26	332.3	5.01	−.09	796	1925	2	22	276.2	5.23	+.01	700
	4	16	339.5	4.99	.10	805		5	13	282.8	5.20	−.01	712
	7	5	346.8	4.98	.10	812		8	1	289.5	5.17	−.02	724
	9	23	354.1	4.96	.11	817		10	20	296.2	5.14	−.03	736
	12	12	1.4	4.96	.11	821	1926	1	8	303.1	5.11	−.05	749
1916	3	1	8.7	4.95	−.11	823		3	29	310.0	5.08	.06	761
	5	20	16.0	4.95	.11	823		6	17	317.0	5.06	.07	772
	8	8	23.3	4.96	.11	821		9	5	324.0	5.04	.08	783
	10	27	30.6	4.96	.11	818		11	24	331.2	5.01	.09	793
1917	1	15	37.9	4.97	−.10	813	1927	2	12	338.4	5.00	−.10	802
	4	5	45.2	4.99	.09	806		5	3	345.6	4.98	.10	810
	6	24	52.4	5.00	.08	798		7	22	352.8	4.97	.11	816
	9	12	59.5	5.02	.07	789		10	10	0.1	4.96	.11	820
	12	1	66.6	5.05	.06	778		12	29	7.5	4.95	.11	823
1918	2	19	73.6	5.07	−.05	767	1928	3	18	14.8	4.95	−.11	824
	5	10	80.6	5.10	.04	755		6	6	22.1	4.95	.11	823
	7	29	87.5	5.12	.02	743		8	25	29.5	4.96	.11	820
	10	17	94.3	5.15	−.01	731		11	13	36.8	4.97	.10	815
1919	1	5	101.0	5.18	0	719	1929	2	1	44.0	4.98	−.09	809
	3	26	107.7	5.21	+.02	707		4	22	51.2	5.00	.09	801
	6	14	114.3	5.24	.03	696		7	11	58.4	5.02	.08	792
	9	2	120.8	5.27	.04	684		9	29	65.5	5.04	.07	782
	11	21	127.2	5.29	.06	674		12	18	72.6	5.06	.05	771

Jupiter's Co-ordinate. (continued)

Date 12^h U.T.			λ_1	$r_1[\cos\beta_1]$	$r_1\sin\beta_1$	$\frac{10^5}{r_1^3}$
			°			
1930	3	8	79.6	5.09	−.04	760
	5	27	86.5	5.11	−.03	748
	8	15	93.3	5.14	−.01	735
	11	3	100.1	5.17	.00	723
1931	1	22	106.8	5.20	+.01	711
	4	12	113.4	5.23	.03	699
	7	1	119.9	5.26	.04	688
	9	19	126.4	5.29	.05	677
	12	8	132.8	5.31	.07	667
1932	2	26	139.1	5.34	+.08	658
	5	16	145.4	5.36	.09	649
	8	4	151.6	5.38	.10	642
	10	23	157.8	5.40	.10	635
1933	1	11	164.0	5.42	+.11	629
	4	1	170.1	5.43	.12	625
	6	20	176.2	5.44	.12	621
	9	8	182.3	5.45	.12	618
	11	27	188.3	5.45	.12	617
1934	2	15	194.3	5.46	+.12	616
	5	6	200.4	5.45	.12	616
	7	25	206.4	5.45	.12	618
	10	13	212.5	5.44	.12	621
1935	1	1	218.6	5.43	+.11	624
	3	22	224.7	5.42	.10	629
	6	10	230.8	5.40	.09	634
	8	29	237.0	5.38	.08	641
	11	17	243.3	5.36	.07	648
1936	2	5	249.6	5.34	+.06	657
	4	25	255.9	5.31	.05	666
	7	14	262.3	5.29	.04	676
	10	2	268.8	5.26	.02	687
	12	21	275.3	5.23	.01	698
1937	3	11	281.9	5.20	.00	710
	5	30	288.6	5.17	−.02	722
	8	18	295.3	5.14	−.03	735
	11	6	302.1	5.12	−.04	747
1938	1	25	309.0	5.09	−.06	759
	4	15	316.0	5.06	.07	771
	7	4	323.1	5.04	.08	782
	9	22	330.2	5.02	.09	792
	12	11	337.4	5.00	.10	802
1939	3	1	344.6	4.98	−.10	809
	5	20	351.9	4.97	.11	816
	8	8	359.2	4.96	.11	821
	10	27	6.5	4.95	.11	824

1910 6 21.5

Fig. 11

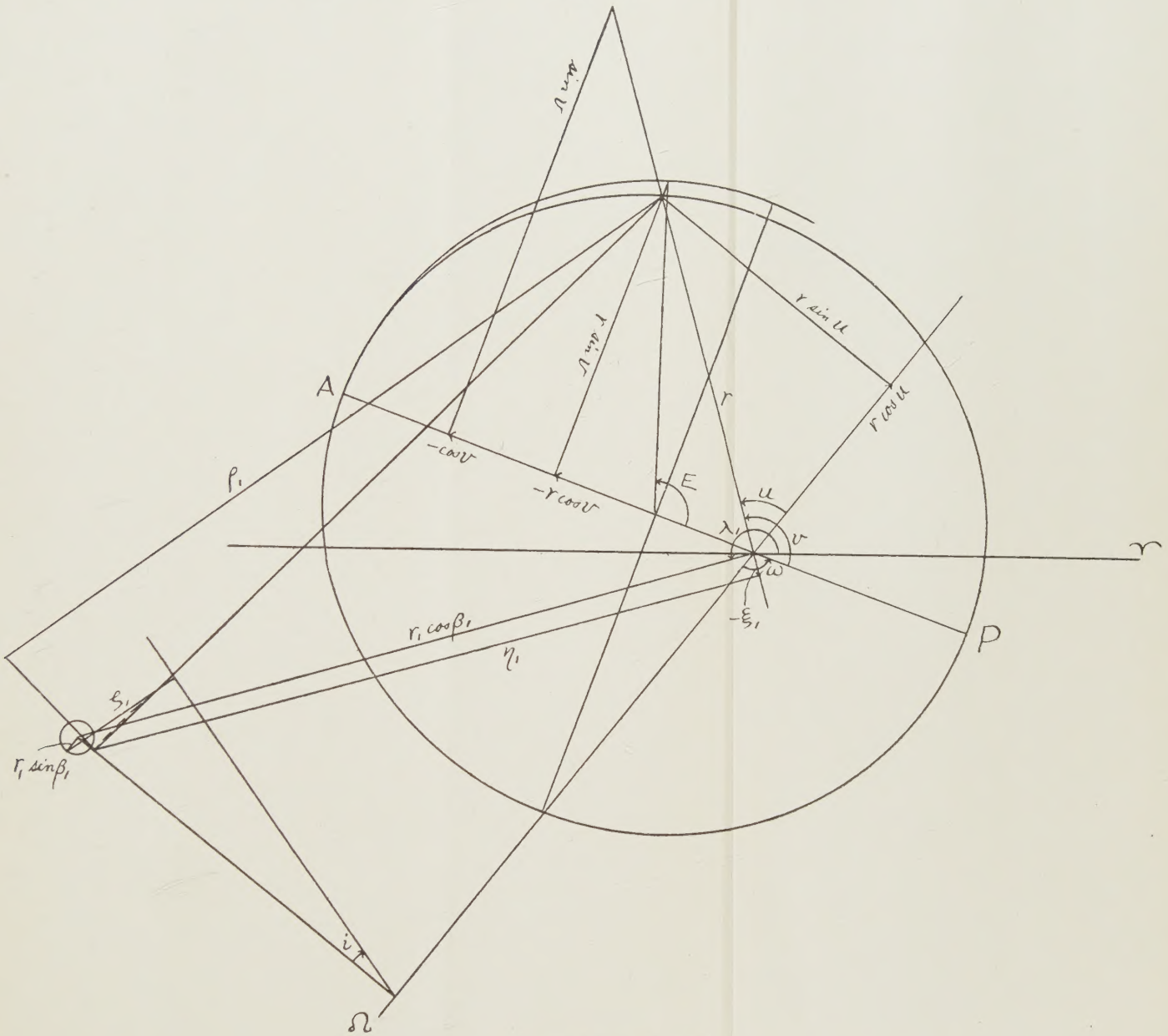

(in the original size)

Vol. XVIII, No. 1, Published Jan. 31, 1935

Price - - - - Yen 1.60

These Memoirs are on Sale at

MARUZEN COMPANY, LTD.

TOKYO, OSAKA, KYOTO, NAGOYA, YOKOHAMA,
FUKUOKA & SENDAI

昭和十年一月二十五日印刷
昭和十年一月三十一日發行

編纂兼發行者　京都帝國大學理學部

印刷者　須磨勘兵衞
京都市下京區北小路通新町西

印刷所　內外出版印刷株式會社
京都市下京區西洞院通七條南

賣捌所　丸善株式會社
東京、大阪、京都、名古屋、横濱、福岡、仙臺

CONTENTS

On the Group of Zero-Sequence
By Toshizô Matsumoto 1
Melting of Metal-Crystals at their Boundaries, and a Theory of Recrystallization of Metals
By Usaburo Yoshida and Kazuo Koyanagi 9
On the Crystal Structure and Crystalline Configuration of the Normal and Modified Si-Al Alloys
By Hajime Kotô 17
An Integral Equation with a Parameter
By Tunezô Satô 35
Graphical Computation of Jupiter's Perturbation on Asteroids
By Joe Ueta 41